





Article

# Carnosine Prevents A $\beta$ -Induced Oxidative Stress and Inflammation in Microglial Cells: A Key Role of TGF- $\beta$ 1

Giuseppe Caruso <sup>1,\*</sup>, Claudia G. Fresta <sup>2,3,†</sup>, Nicolò Musso <sup>4</sup>, Mariaconcetta Giambirtone <sup>1</sup>, Margherita Grasso <sup>1,5</sup>, Simona F. Spampinato <sup>6</sup>, Sara Merlo <sup>6</sup>, Filippo Drago <sup>6</sup>, Giuseppe Lazzarino <sup>7</sup>, Maria A. Sortino <sup>6</sup>, Susan M. Lunte <sup>2,3,8</sup> and Filippo Caraci <sup>1,5,\*</sup>

<sup>1</sup> Oasi Research Institute—IRCCS, 94018 Troina, Italy; mcgiambirtone@oasi.en.it (M.G.); grassomargherita940@gmail.com (M.Gr.)

<sup>2</sup> Ralph N. Adams Institute for Bioanalytical Chemistry, University of Kansas, Lawrence, KS 66047-1620, USA; forclaudiafresta@gmail.com (C.G.F.); slunte@ku.edu (S.M.L.)

<sup>3</sup> Department of Pharmaceutical Chemistry, University of Kansas, Lawrence, KS 66047-1620, USA

<sup>4</sup> Bio-nanotech Research and Innovation Tower (BRIT), University of Catania, 95125 Catania, Italy; nmusso@unict.it

<sup>5</sup> Department of Drug Sciences, University of Catania, 95125 Catania, Italy

<sup>6</sup> Department of Biomedical and Biotechnological Sciences, Section of Pharmacology, University of Catania, 95125 Catania, Italy; simona\_spampinato@hotmail.com (S.F.S.); sara\_merlo@hotmail.com (S.M.); f.drago@unict.it (F.D.); msortino@unict.it (M.A.S.)

<sup>7</sup> Department of Biomedical and Biotechnological Sciences, Division of Medical Biochemistry, University of Catania, 95125 Catania, Italy; lazzarig@unict.it

<sup>8</sup> Department of Chemistry, University of Kansas, Lawrence, KS 66047-1620, USA

\* Correspondence: forgiuseppecaruso@gmail.com (G.C.); carafil@hotmail.com (F.C.); Tel.: +39-093-593-6111 (G.C.); +39-095-738-4251 (F.C.); Fax: +39-093-565-3327 (G.C.); +39-095-738-4238 (F.C.)

† Current address: Department of Biomedical and Biotechnological Sciences, PhD Program in Neurosciences, University of Catania, 95125 Catania, Italy.

Received: 28 December 2018; Accepted: 14 January 2019; Published: 17 January 2019



**Abstract:** Carnosine ( $\beta$ -alanyl-L-histidine), a dipeptide, is an endogenous antioxidant widely distributed in excitable tissues like muscles and the brain. Carnosine is involved in cellular defense mechanisms against oxidative stress, including the inhibition of amyloid-beta (A $\beta$ ) aggregation and the scavenging of reactive species. Microglia play a central role in the pathogenesis of Alzheimer's disease, promoting neuroinflammation through the secretion of inflammatory mediators and free radicals. However, the effects of carnosine on microglial cells and neuroinflammation are not well understood. In the present work, carnosine was tested for its ability to protect BV-2 microglial cells against oligomeric A $\beta$ 1-42-induced oxidative stress and inflammation. Carnosine prevented cell death in BV-2 cells challenged with A $\beta$  oligomers through multiple mechanisms. Specifically, carnosine lowered the oxidative stress by decreasing NO and O $_2$ <sup>-•</sup> intracellular levels as well as the expression of iNOS and Nox enzymes. Carnosine also decreased the secretion of pro-inflammatory cytokines such as IL-1 $\beta$ , simultaneously rescuing IL-10 levels and increasing the expression and the release of TGF- $\beta$ 1. Carnosine also prevented A $\beta$ -induced neurodegeneration in mixed neuronal cultures challenged with A $\beta$  oligomers, and these neuroprotective effects were completely abolished by SB431542, a selective inhibitor of the type-1 TGF- $\beta$  receptor. Our data suggest a multimodal mechanism of action of carnosine underlying its protective effects on microglial cells against A $\beta$  toxicity with a key role of TGF- $\beta$ 1 in mediating these protective effects.

**Keywords:** carnosine; microglia; Alzheimer's disease; neurodegeneration; neuroinflammation; reactive oxygen and nitrogen species; oxidative stress; TGF- $\beta$ 1

## 1. Introduction

Carnosine ( $\beta$ -alanyl-L-histidine) is a natural dipeptide widely distributed in mammalian tissues [1,2] and exists at particularly high concentrations (millimolar order) in the brain as well as in skeletal and cardiac muscles (up to 20 mM). Carnosine has been shown to be neuroprotective through different mechanisms: the prevention of oxidative stress [3], reduction of intraneuronal amyloid- $\beta$  ( $A\beta$ ) accumulation, mitochondrial dysfunctions and cognitive deficits in 3xTg-AD mice [4], as well as the inhibition of  $A\beta$  aggregation [5], modulation of macrophage nitric oxide (NO) production and pro-/anti-inflammatory (M1/M2) ratio [6]. Furthermore, it is also able to scavenge the superoxide ion ( $O_2^{\bullet-}$ ) [7] and other reactive species [8].

$A\beta$  is a 42 amino acids long ( $A\beta_{1-42}$ ) peptide physiologically present in the brain and cerebrospinal fluid of human beings [9]. Together with marked inflammation [10], both the extracellular deposition of insoluble aggregates of this peptide in the brain and its blood vessels [11,12] and the formation of neurofibrillary tangles composed by the highly phosphorylated form of tau protein [13] represent the neuropathological hallmarks of Alzheimer's disease (AD).  $A\beta$  peptide can undergo aggregation through a step-by-step process, starting with soluble monomers and evolving to the formation of oligomers, protofibrils, and mature fibrils [14], with the oligomeric structures representing the more toxic species [15].

Microglia are a subtype of brain glial cells and constitute up to 10% of all cells in the healthy human cortex [16]. These cells are in intimate contact with neurons and are involved in many basic physiological processes [17]. Microglial cells, often found near  $A\beta$  plaques in AD patients [18], are able to produce various neurotrophic and anti-inflammatory factors essential for cell growth and protection; they can also release different cytotoxic substances, such as reactive oxygen species (ROS) and reactive nitrogen species (RNS), and pro-inflammatory cytokines such as IL-1 $\beta$ , IL-6, and TNF- $\alpha$  [17]. All the above substances are strongly connected to AD pathogenesis and amyloid-related neurodegeneration [19].

NO (RNS species) and  $O_2^{\bullet-}$  (ROS species) are part of the natural aerobic metabolism of cells and are involved in many physiological and pathological processes [20,21]. Peroxynitrite, the reaction product between NO and  $O_2^{\bullet-}$ , can react and consequently damage fatty acids, proteins, DNA, and mitochondria leading to oxidative and nitrosative stress [22], inflammation [23], and then neurodegenerative phenomena [24,25]. During the inflammation process, both inducible nitric oxide synthase (iNOS), responsible for NO production [26,27], and NADPH oxidase (Nox), responsible for  $O_2^{\bullet-}$  production [28], are overactivated in immune cells such as macrophage and microglia [20,29,30]. When simultaneously activated, iNOS and Nox act synergistically to promote neuronal death through the generation of peroxynitrite, which is a more dangerous species if compared with NO and/or  $O_2^{\bullet-}$  [31]. Mediators of cytotoxicity released from activated microglia also include arachidonic acid, glutamate, and histamine [32]. Furthermore, it has been shown that macrophages and microglia play a crucial role in several diseases characterized by oxidative stress and inflammation and also that the modulation of their pro-/anti-inflammatory (M1/M2) ratio and secretion products might represent a novel pharmacological approach for the treatment of these disorders [33,34].

Neuroinflammation is a widely accepted factor associated with the pathogenesis of AD [35]. Different cell types, including microglia, shift from the resting to activated state during the neuroinflammation process [36], producing a higher amount of pro-inflammatory cytokines such as TNF- $\alpha$ , IL-1 $\beta$ , and IL-6 [19]. Activated microglia have been shown to contribute to the development and progression of neurodegenerative disorders [37] and the presence of both reactive microglia and astrocytes has been observed in association with amyloid accumulation in AD brain [38]. However, activated microglia are also able to produce anti-inflammatory mediators [39]. Among these molecules, the multifunctional cytokine TGF- $\beta$ 1 has been shown to play a pivotal role in AD, exerting neuroprotective effects against  $A\beta$ -induced neurodegeneration [40,41]. Furthermore, the secretion of TGF- $\beta$ 1 from peripheral blood mononuclear cells in the circulation [42] along with the levels of TGF- $\beta$ 1 in the plasma [43] are reduced in AD subjects. Lastly, Wyss-Coray et al. showed that TGF- $\beta$ 1

promoted microglial A $\beta$  clearance and the reduction of plaque burden in AD mice and enhanced A $\beta$  clearance by BV-2 microglial cells [44], suggesting a link between microglia activity, TGF- $\beta$ 1 release, and the neuroprotective activity of this neurotrophic factor against A $\beta$ -induced toxicity.

In the present study, we first investigated the toxicity and the production of NO and O $_2^{\bullet-}$  induced by different concentrations of A $\beta$ 1-42 oligomers, in the absence or in the presence of carnosine, in BV-2 cells, an established experimental model for mimicking neuroinflammation in primary microglia [45]. Additionally, in order to understand the molecular mechanisms underlying the ability of carnosine in decreasing the production of molecules related to oxidative and nitrosative stresses, we studied the expression of iNOS and Nox enzymes along with the expression and secretion of pro- and anti-inflammatory cytokines in BV-2 cells challenged with A $\beta$ 1-42 oligomers. Lastly, the protective activity of carnosine, as well as the role played by TGF- $\beta$ 1 in preventing A $\beta$ -induced neuronal death, was evaluated in mixed neuronal cultures.

The evidence that carnosine exerts protective effects by decreasing A $\beta$ 1-42-induced toxicity in microglial cells, counteracting the oxidative stress and the inflammation status, is presented.

## 2. Material and Methods

### 2.1. Materials and Reagents

Microglial BV-2 cells (ICLC ATL03001) were purchased from Interlab Cell Line Collection (ICLC, Genova, Italy). HFIP-treated amyloid  $\beta$ -peptide (1-42) was obtained from Bachem Distribution Services GmbH (Weil am Rhein, Germany). DMEM/F12 (1:1) medium, RPMI-1640 medium, phenol red-free RPMI-1640 medium, trypsin-EDTA solution (0.25% Trypsin/0.53 mM EDTA in HBSS without calcium or magnesium), fetal bovine serum (FBS), and penicillin–streptomycin antibiotic solution were purchased from American Type Culture Collection (ATCC) (Manassas, VA, USA). L-Carnosine, anhydrous dimethyl sulfoxide (DMSO), trypan blue solution, glucose, cytosine-D-araboside, sodium dodecyl sulfate (SDS), MTT [3-(4,5-dimethylthiazol-2-yl)-2,5-diphenyltetrazolium bromide] tetrazolium salt, and phosphate-buffered saline (PBS) were all supplied by Sigma Aldrich (St. Louis, MO, USA). Agilent DNA 1000 Kit was obtained from Agilent (Santa Clara, CA, USA). The 4-amino-5-methylamino-2',7'-difluorofluorescein diacetate (DAF-FM DA) and MitoSOX Red probes were purchased from Life Technologies (Carlsbad, CA, USA). Platinum Taq DNA Polymerase, SuperScript<sup>TM</sup> II Reverse Transcriptase, SuperScript III First-Strand Synthesis SuperMix, dNTP Set, TE buffer, GlutaMAX Supplement, 25 and 75 mL polystyrene culture flasks, 12-, 48-, and 96-well plates, ethanol (95%), sodium hydroxide, boric acid, hydrochloric acid, horse serum, fetal calf serum (FCS), and C-Chip disposable hemocytometers were obtained from Thermo Fisher Scientific (Thermo Fisher Waltham, MA, USA). QuantiTect SYBR Green PCR Kits, RNeasy Mini Kit, QuantiTect Primer Assays, and Custom Multi-Analyte ELISArray Kit were purchased from Qiagen (Hilden, Germany). Eppendorf LoBind 1.5 ml Microcentrifuge Tubes PCR Clean and PCR tubes were both supplied by Eppendorf (Hamburg, Germany). Polyethersulfone membrane (3 kDa) centrifuge filters were purchased from VWR International (West Chester, PA, USA). The specific inhibitor of type1 TGF- $\beta$ 1 receptor 4-[4-(1,3-benzodioxol-5-yl)-5-(2-pyridinyl)-1Himidazol-2-yl]benzamide (SB431542) was obtained from the R&D system (Minneapolis, MN, USA). Polydimethylsiloxane (PDMS) microdevices were prepared from a Sylgard 184 elastomer kit (Ellsworth Adhesives, Germantown, WI, USA). Highest Grade Mica Sheets V1 were purchased from Ted Pella Inc (Redding, CA, USA). All water used was ultrapure (18.3 M $\Omega$  cm) (Milli-Q Synthesis A10, Millipore, Burlington, MA, USA).

### 2.2. Preparation of A $\beta$ 1-42 Oligomers

A $\beta$ 1-42 oligomers (oA $\beta$ 1-42) were prepared as previously described in details elsewhere [46]. In brief, the lyophilized HFIP-treated A $\beta$ 1-42 monomers were first suspended in DMSO and then diluted in an ice-cold cell culture medium DMEM/F12 (1:1) at the final concentration of 100  $\mu$ M. Next, the A $\beta$ 1-42 samples (100  $\mu$ M) were incubated in the absence (oA $\beta$ 1-42) or presence (A $\beta$ 1-42 + Car

(co-inc.) of carnosine at the final concentration of 1 mM for 72 h at 4 °C. After this incubation step, the two (without or with carnosine) A $\beta$ 1-42 samples were immediately used or aliquoted and stored at –20 °C until use.

### 2.3. Atomic Force Microscope (AFM)

Amyloid oligomer formation was verified by AFM (Supplementary Figure S1A).

AFM images were collected by using dynamic scanning force microscopy in the air, using a WITec ALPHA300 RS Confocal Raman AFM combined microscope (LOT-QuantumDesign GmbH, Darmstadt, Germany) and etched-silicon probes (Nanosensors, Neuchâtel, Switzerland) with a pyramidal-shaped tip having a radius of curvature <10 nm and a nominal internal angle of 35°. A total of 5  $\mu$ L of each individual A $\beta$ 1-42 sample (oA $\beta$ 1-42 or A $\beta$ 1-42 + Car (co-inc.)) were adsorbed onto the mica and analyzed directly by sensing the adsorbed material with a microfabricated silicon tip attached to a sensitive cantilever. The resulting relief map was subsequently converted into a visual image.

### 2.4. Cell Culture and Preparation

#### 2.4.1. BV-2 Cells

BV-2 cells were cultured in an RPMI-1640 medium enriched with heat-inactivated FBS (10% *v/v*), L-glutamine (2 mM), streptomycin (0.3 mg mL<sup>-1</sup>), and penicillin (50 IU mL<sup>-1</sup>). The cells were cultured in 75 mL polystyrene culture flasks at a density of 5 × 10<sup>6</sup> cells/flask, maintained in a humidified environment at 37 °C and 5% CO<sub>2</sub>/95% air atmosphere, and passaged every 3–5 days depending on the cell confluence in order to avoid cell overgrowth. The day prior to treatment, cells were harvested using a 2.5 mL of trypsin-EDTA solution, counted with a C-Chip disposable hemocytometer, and seeded in 5 mL culture flasks, 12-, or 48-well plates at the appropriate density. Prior to the beginning of each experiment, the exact number of live BV-2 cells necessary for cell seeding was determined by using the trypan blue exclusion assay. For each cell count, 50  $\mu$ L of cell suspension was diluted 1:2 to 1:5 (based on cell density) with a 0.4% trypan blue solution.

#### 2.4.2. Mixed Neuronal Cultures

Mixed neuronal cultures were obtained from rats at embryonic day 15 (Harlan Laboratories, Italy) as previously described [46,47]. Cells were grown into DMEM/F12 (1:1) and enriched with 10% horse serum, 10% FCS, 2 mM glutamine, and 6 mg/ml glucose. After 7–10 days *in vitro*, to avoid the proliferation of non-neuronal elements, cytosine-D-arabinoside (at the final concentration of 10  $\mu$ M) was added to the cultures for 3 days. Cells were then moved into a maintenance serum-free medium. As soon as the right confluence was reached, cells were treated with A $\beta$  oligomers (2  $\mu$ M) for 48 h both in the presence or in the absence of increasing concentrations of carnosine (1, 5, and 10 mM). The possible neuroprotective activity against A $\beta$ 1-42-induced toxicity played by TGF- $\beta$ 1 was indirectly investigated by using the specific inhibitor of type-1 TGF- $\beta$  receptor, SB431542, at 10  $\mu$ M as previously accomplished [46].

### 2.5. Measurement of Cell Viability and Cell Death by the MTT and Trypan Blue Exclusion Assays

The effect on the BV-2 cells viability of the treatment with different concentrations (1, 5, and 10  $\mu$ M) of A $\beta$ 1-42 oligomers for 24 h as well as the possible protective effects of carnosine in counteracting A $\beta$ 1-42-induced toxicity (A $\beta$ 1-42 + Car (co-inc.) or BV-2 cells simultaneously treated with already formed A $\beta$ 1-42 oligomers and carnosine (oA $\beta$ 1-42 + Car (co-treat.)) were measured through the MTT assay as previously reported [48,49]. Briefly, BV-2 cells were seeded in 48-well plates at the density of 1.5 × 10<sup>5</sup> cells/well. A total of 24 h after cell treatment the medium from each well was removed and the MTT solution (1 mg/mL in RPMI-1640 medium) was added. Following 2 h of incubation at 37 °C and 5% CO<sub>2</sub>/95% air atmosphere, the MTT solution was removed and the formed crystals were dissolved with DMSO. Lastly, 200  $\mu$ L of each well were transferred to a 96-well plate and the

absorbance at 569 nm was read using a plate reader (Spectra Max M5, Molecular Devices, Sunnyvale, CA, USA). Resting (untreated) cells were used as controls.

The toxicity induced in mixed neuronal cultures 48 h after A $\beta$ 1-42 oligomers treatment was quantitatively assessed by trypan blue exclusion assay [46,47]. Cell counts were performed in three to four random microscopic fields/well.

#### 2.6. NO and O $_2^{\bullet-}$ Production Determination Using DAF-FM DA and MitoSOX Red Probes

The experiments carried out to investigate the production of NO and O $_2^{\bullet-}$  were performed as described previously [50] with slight modifications. BV-2 cells previously seeded in 5 mL culture flasks ( $5 \times 10^6$  cells) were treated for 24 h. At the end of the cell treatment, in order to analyze intracellular NO and O $_2^{\bullet-}$  production, the cells were washed three times with cold PBS (0.01 M, pH 7.4) and then incubated with a phenol red free RPMI-1640 medium containing DAF-FM DA or MitoSOX Red probes previously prepared in 99% sterile DMSO for 1 h. During the incubation time, each flask was covered with aluminum foil to minimize any photobleaching of the probes. Next, the BV-2 cells were harvested, counted, and centrifuged ( $1137 \times g$  for 4 min). The obtained cell pellet was washed three times with cold PBS (0.01 M, pH 7.4), lysed using 50  $\mu$ L of pure ethanol, centrifuged ( $18.690 \times g$  for 10 min), and filtered with a polyethersulfone membrane (3 kDa) centrifuge filter. Then 10  $\mu$ L of each filtered cell lysate was added to a 90  $\mu$ L solution consisting of 10 mM boric acid and 7.5 mM SDS at pH 9.2 and transferred to a 96-well plate where the fluorescence was read using a plate reader (Spectra Max M5). Resting cells were used as controls.

In order to detect the real fluorescence due to the reaction between the probes (DAF-FM DA or MitoSOX Red) and the molecules of interest (NO or O $_2^{\bullet-}$ ), and to discriminate our compounds from (if any) other fluorescent side products, at least one sample for each experimental condition was run using microchip electrophoresis with laser-induced fluorescence (ME-LIF). The fabrication of PDMS microdevices [51,52], as well as the experimental conditions (sample injection, separation, and detection), data acquisition, and data analysis employed to carry out the ME-LIF experiments, have been described previously [6]. Briefly, a 4" diameter silicon wafer was coated with SU-8 10 negative photoresist to a thickness of 15  $\mu$ m with a Cee 100 spincoater (Brewer Science Inc., Rolla, MO, USA). The obtained wafer was soft baked in two steps (65  $^{\circ}$ C for 2 min and 95  $^{\circ}$ C for 5 min) using a programmable hotplate (Thermo Scientific, Asheville, NC, USA). Microchip designs were drawn with AutoCAD (Autodesk Inc., San Rafael, CA, USA) and printed onto a transparency film (Infinite Graphics Inc., Minneapolis MN, USA). The coated wafer was covered with a transparency film mask and exposed to UV light (ABM Inc., San Jose, CA, USA). The wafer was then post-baked in two steps (65  $^{\circ}$ C for 2 min and 95  $^{\circ}$ C for 10 min). After the post-bake, the wafer was developed in SU-8 developer, rinsed, and dried. Lastly, the wafer underwent a hard bake at 180–200  $^{\circ}$ C for 2 h. The final silicon master contained 15  $\mu$ m thick and 40  $\mu$ m wide microchannels. In order to complete the final hybrid PDMS-glass microchip device, the PDMS layer was sealed to a borofloat glass plate. Prior to each cell lysate analysis, the PDMS-glass device was flushed with NaOH (0.1 M for 5 min) and a running buffer (10 mM boric acid, 7.5 mM SDS at pH 9.2 for 5 min). Each separation was performed using a 30 kV high voltage power supply (Ultravolt, Ronkonkoma, NY, USA). A total of +2400 V and +2200 V were applied to the running buffer reservoir and sampling reservoir, respectively. The sample was introduced into the separation channel using a 1-s gated injection. To avoid the presence of any residual sample on the channels, the system was flushed for 60 s with a running buffer after each sample analysis. Excitation, detection, data acquisition, and data analysis were carried out using the same technologies and programs already described [6].

A schematic representation of the different steps of the chip manufacturing process, the various components needed for ME-LIF experiments, as well as a representative electropherogram, obtained running a cell sample lysate for NO and O $_2^{\bullet-}$  detection, are shown in Supplementary Figure S2.

### 2.7. Gene Expression Analysis by Quantitative Real-Time PCR (qRT-PCR)

The total RNA was extracted using the commercial RNeasy Mini Kit according to the manufacturer's recommendations. The concentration of total RNA recovered from  $3.5 \times 10^5$  cells (previously seeded in 12-well plates) treated for 6 h was determined by measuring the absorbance at 260 nm with a Varioskan®Flash spectrophotometer (Thermo Fisher Scientific, Waltham, MA, USA). Reverse transcription was performed using 100 ng of total RNA, RNaseH reverse transcriptase, and random primer hexamers (Superscript II, Thermo Fisher Scientific). Next, each sample was quantified, diluted to a final concentration of 25 ng/μL, and used for qRT-PCR analysis (LightCycler®480 System, Roche Molecular Systems, Inc., Pleasanton, CA, USA). The QuantiTect Primer Assays (Qiagen) employed for the gene expression analysis along with the official name, official symbol, alternative titles/symbols, detected transcript, amplicon length, and primers catalog number are shown in Table 1.

**Table 1.** The list of primers used for quantitative real-time PCR (qRT-PCR).

Official Name #	Official Symbol	Alternative Titles/Symbols	Detected Transcript	Amplicon Length	Cat. No. §
nitric oxide synthase 2, inducible	Nos2	iNOS; Nos-2; Nos2a; i-NOS; NOS-II; MAC-NOS	NM_010927	118 bp	QT00100275
NADPH oxidase 1	Nox1	MOX1; NOH1; NOH-1; NOX1a; Nox-1; GP91-2; NOX1alpha	NM_172203 XM_006528515	180 bp	QT00140091
cytochrome b-245, beta polypeptide	Cybb	Cgd; Cyd; Nox2; C88302; gp91-1; gp91phox; CGD91-phox	NM_007807 XM_006527565	146 bp	QT00139797
transforming growth factor, beta 1	Tgfb1	Tgfb; Tgfb-1; TGFbeta1; TGF-beta1	NM_011577	145 bp	QT00145250
interleukin 6	Il6	Il-6	NM_031168	128 bp	QT00098875
glyceraldehyde-3-phosphate dehydrogenase	Gapdh	Gapd	NM_008084 XM_001003314 XM_990238 NM_001289726	144 bp	QT01658692

# <https://www.ncbi.nlm.nih.gov/gene/>. § <https://www.qiagen.com/it/shop/pcr/real-time-pcr-enzymes-and-kits/two-step-qrt-pcr/quantitect-primer-assays/>.

qRT-PCR amplifications were performed in quadruplicate using a mixture of SYBR Green PCR Master Mix (Thermo Fisher Scientific), cDNA samples (100 ng), and specific primers (total reaction volume of 10 μL). Amplification conditions included a first cycle at 95 °C (10 min) followed by 50 cycles at 95 °C (10 seconds), and a final cycle at 60 °C (30 seconds). As a negative control, a reaction in the absence of cDNA (no template control, NTC) was performed and verified by using an Agilent Bioanalyzer 2100 with Agilent DNA 1000 Kit. The relative RNA expression level for each sample was calculated using the  $2^{-\Delta\Delta CT}$  method [53,54] by comparing the threshold cycle (CT) value of the gene of interest to the CT value of our selected internal control (GAPDH gene).

### 2.8. Cytokine Secretion

Cytokines quantification in cell culture supernatants was carried out by using a Custom Multi-Analyte ELISArray Kit according to the manufacturer's instructions. Briefly, BV-2 cells previously seeded in 48-well plates at the density of  $1.5 \times 10^5$  cells/well were treated for 24 h and the supernatant from each well was collected, centrifuged at  $1000 \times g$  for 10 min in order to remove any particulate material, and assayed immediately or stored at  $-80$  °C. A total of 50 μL of assay buffer and 50 μL of samples or control samples were added into the appropriate wells of the ELISArray plate and incubated for 2 h at room temperature (RT). After washing 3 times with Wash Buffer, 100 μL of Detection Antibody Solution was added to each well pursued by the following steps: 1 h incubation, 3 washes, the addition of 100 μL Avidin-HRP Conjugate, 30 min incubation at RT, 4 washes, the

addition of a 100  $\mu$ L Development Solution, and 15 min incubation at RT under the dark. As a final step, 100  $\mu$ L of Stop Solution was added to each well and the absorbance at 450 nm was read using a Synergy H1 Hybrid Multi-Mode Microplate Reader (Biotek, Shoreline, WA, USA) within 30 min of stopping the reaction. As suggested by the vendor, in order to detect the real absorbance, wavelength correction was applied, subtracting the readings at 570 nm from the reading at 450 nm.

### 2.9. Statistical Analysis

Statistical analysis was performed using GraphPad Prism (GraphPad software, San Diego, CA, USA). The within-group comparison was performed by the one-way analysis of variance (ANOVA). The *post hoc* Tukey test was used for multiple comparisons.

### 2.10. Study Approval

The study in mixed neuronal cultures was authorized by the Institutional Animal Care and Use Committee (IACUC) of the University of Catania (OPBA Project #169/2015). Animal care followed Italian (D.M.116192) and EEC (O.J. of E.C. L 358/1 12/18/1986) regulations on the protection of animals used for experimental and scientific purposes.

## 3. Results

### 3.1. Carnosine Protects BV-2 Cells Against A $\beta$ 1-42 Oligomers-Induced Cell Death

The first aim of the present study was to evaluate the toxicity induced by increasing concentrations of A $\beta$ 1-42 oligomers (oA $\beta$ 1-42) (1, 5, and 10  $\mu$ M) on microglial BV-2 cells. Data illustrated in Figure 1 show that the treatment of BV-2 cells for 24 h with increasing concentrations of oA $\beta$ 1-42 provoked a dose-dependent decrease in cell viability.

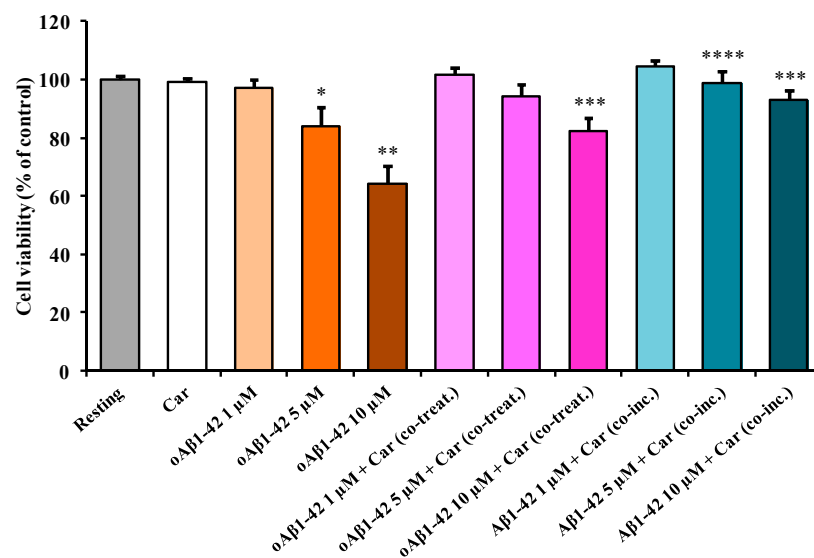


**Figure 1.** The change in the cell viability caused by challenging BV-2 cells with oA $\beta$ 1-42 and the protective effects of carnosine. BV-2 cells were treated for 24 h with increasing oA $\beta$ 1-42 concentrations (1, 5, or 10  $\mu$ M), in the absence or presence of carnosine (Car, 1 mM) (oA $\beta$ 1-42 + Car (co-treat.)), or with a solution consisting of A $\beta$ 1-42 monomers previously incubated in the presence of carnosine (1 mM) during the oligomerization process (A $\beta$ 1-42 + Car (co-inc.)); for more details see “Material and Methods” section. Data are the mean ( $n = 4$ ) of 5 independent experiments and are expressed as the percent variation with respect to the viability recorded in resting (control) cells. Standard deviations are represented by vertical bars. \* Significantly different from resting cells,  $p < 0.01$ , \*\* significantly different from resting cells,  $p < 0.001$ , \*\*\* significantly different from corresponding treatment with no carnosine,  $p < 0.001$ , \*\*\*\* significantly different from corresponding treatment with no carnosine,  $p < 0.01$ .

Unlike 1  $\mu\text{M}$  oA $\beta$ 1-42 (−3% in cell viability, not significant), the treatment with 5  $\mu\text{M}$  oA $\beta$ 1-42 led to a significant toxic effect (−19% in cell viability,  $p < 0.01$  compared to the resting cells). As expected, the stronger decrease in cell viability (−36%,  $p < 0.001$  compared to the resting cells) was observed after the treatment with 10  $\mu\text{M}$  oA $\beta$ 1-42. In order to examine the protective effects of carnosine, BV-2 cells were treated simultaneously with oA $\beta$ 1-42 and carnosine (oA $\beta$ 1-42 + Car (co-treat.)). Figure 1 clearly shows that the BV-2 cells' viability significantly increased in the presence of carnosine when compared to treatment with the increasing concentrations of oA $\beta$ 1-42 (1, 5, and 10  $\mu\text{M}$ ). A maximal protective effect was observed for cells treated simultaneously with oA $\beta$ 1-42 10  $\mu\text{M}$  and carnosine (+18% in cell viability,  $p < 0.001$  compared to the corresponding treatment with no carnosine). As a part of our toxicity studies, we also challenged BV-2 cells with a solution consisting of A $\beta$ 1-42 monomers previously incubated with carnosine during the oligomerization process (A $\beta$ 1-42 + Car (co-inc.)). This set of experiments was purposely designed in order to determine whether the well-know anti-aggregation property of carnosine contributed to increasing the cell viability counteracting oA $\beta$ 1-42 formation and then preventing A $\beta$  toxicity. Considering the presence of carnosine during the oligomerization process, both treatments 5  $\mu\text{M}$  A $\beta$ 1-42 + Car (co-inc.) and 10  $\mu\text{M}$  A $\beta$ 1-42 + Car (co-inc.) showed cell viability values significantly higher (+15%,  $p < 0.01$  and +29%,  $p < 0.001$ , respectively) compared to the corresponding treatment with no carnosine.

### 3.2. Carnosine Decreases A $\beta$ 1-42-Induced NO Production in Cultured Microglial Cells

Figure 2 shows the effect of A $\beta$ 1-42 treatment on the intracellular NO production in BV-2 cells.

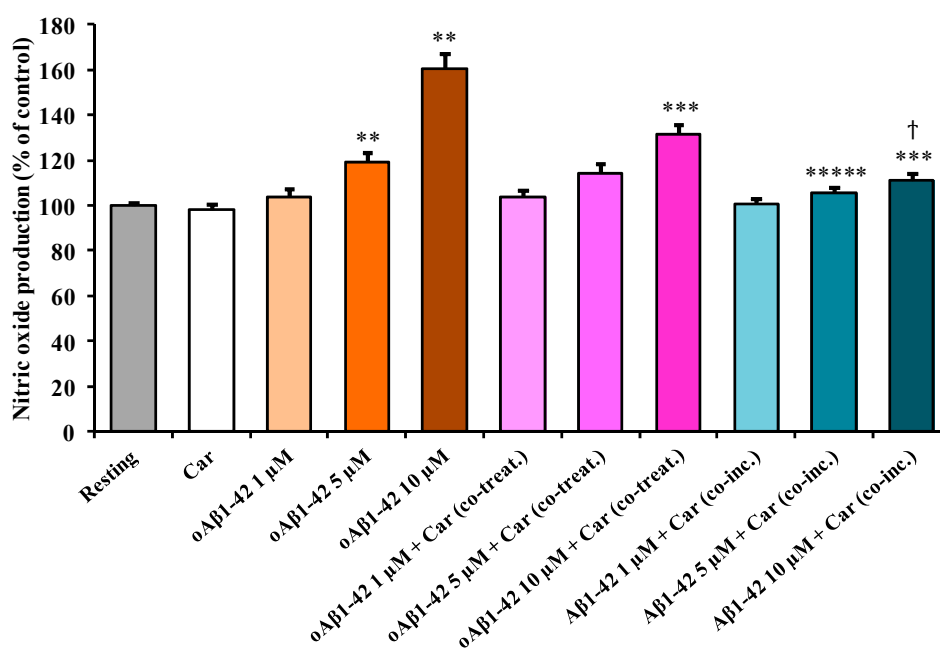


**Figure 2.** The change in the NO production induced by treating BV-2 cells with A $\beta$ 1-42 and effects of carnosine. BV-2 cells were treated for 24 h with increasing oA $\beta$ 1-42 concentrations (1, 5, or 10  $\mu\text{M}$ ), in the absence or presence of carnosine (Car, 1 mM) (oA $\beta$ 1-42 + Car (co-treat.)), or with a solution consisting of A $\beta$ 1-42 monomers previously incubated in the presence of carnosine (1 mM) during the oligomerization process (A $\beta$ 1-42 + Car (co-inc.)). Data are the mean of 5 independent experiments and are expressed as the percent variation with respect to the NO production recorded in resting cells. Standard deviations are represented by vertical bars. \*\* Significantly different from resting cells,  $p < 0.001$ , \*\*\* significantly different from corresponding treatment with no carnosine,  $p < 0.001$ , \*\*\*\* significantly different from corresponding treatment with no carnosine,  $p < 0.05$ , † significantly different from cells treated with 10  $\mu\text{M}$  oA $\beta$ 1-42 + Car (co-treat.),  $p < 0.001$ .



This increase in NO production was significant in the case of both 5  $\mu\text{M}$  oA $\beta$ 1-42 (+19%,  $p < 0.001$  compared to resting cells) and 10  $\mu\text{M}$  oA $\beta$ 1-42 (+60%,  $p < 0.001$  compared to resting cells) treatments. The addition of carnosine to the resting BV-2 cells did not cause any significant change in the basal microglia NO production. To test the effect of carnosine on NO production in stimulated BV-2 cells, carnosine was added along with three different concentrations of oA $\beta$ 1-42. The amount of NO production was essentially the same for cells treated with 1  $\mu\text{M}$  oA $\beta$ 1-42, in the presence or absence of carnosine. A slight, but not significant, decrease (−5%) was measured in 5  $\mu\text{M}$  oA $\beta$ 1-42 + Car (co-treat.) compared to cells stimulated in the absence of carnosine. The production due to the treatment with 10  $\mu\text{M}$  oA $\beta$ 1-42 was significantly lowered by the presence of carnosine (−29%,  $p < 0.001$ ). As for 1  $\mu\text{M}$  oA $\beta$ 1-42 + Car (co-treat.), the production of NO for A $\beta$ 1-42 1  $\mu\text{M}$  + Car (co-inc.) treatment was comparable to the one detected in the resting cells. The presence of carnosine during the oligomerization process strongly decreased the effect of A $\beta$ 1-42 in inducing NO production. In fact, both 5  $\mu\text{M}$  A $\beta$ 1-42 + Car (co-inc.) (−14%,  $p < 0.05$ ) and 10  $\mu\text{M}$  A $\beta$ 1-42 + Car (co-inc.) (−49%,  $p < 0.001$ ) treatments showed a significant decrease in NO production when compared with the corresponding treatment in the absence of carnosine. Interestingly, the production of NO for the 10  $\mu\text{M}$  A $\beta$ 1-42 + Car (co-inc.) treatment was significantly lower than 10  $\mu\text{M}$  oA $\beta$ 1-42 + Car (co-treat.) (−20 %,  $p < 0.001$ ).

### 3.3. Carnosine Decreases A $\beta$ 1-42-Induced $\text{O}_2^{\bullet-}$ Production in Cultured Microglial Cells

Figure 3 depicts the effect of A $\beta$ 1-42 treatment on the intracellular  $\text{O}_2^{\bullet-}$  production in BV-2 cells.

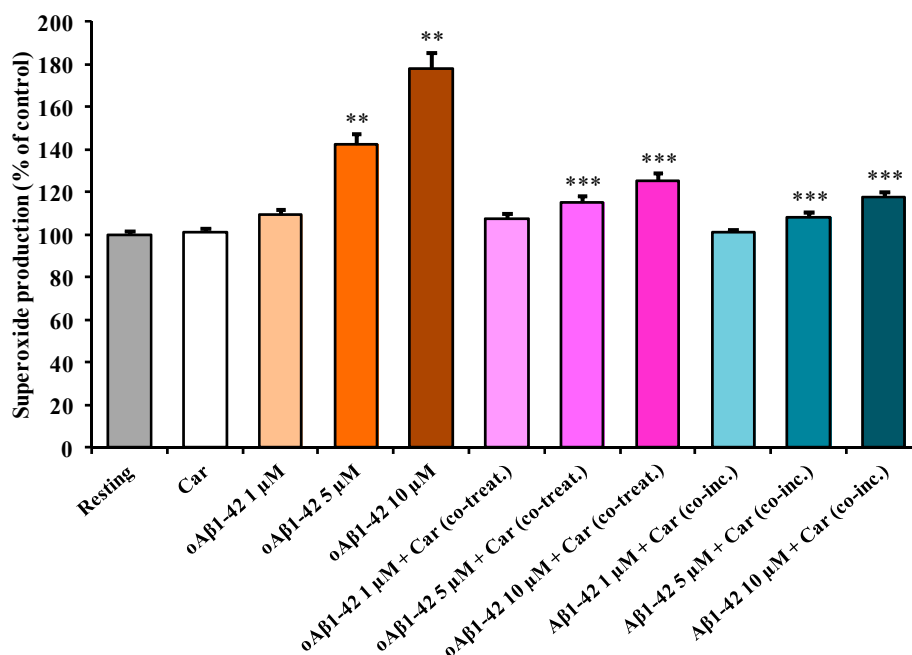


**Figure 3.** The change in  $\text{O}_2^{\bullet-}$  production induced by treating BV-2 cells with A $\beta$ 1-42 and effects of carnosine. BV-2 cells were treated for 24 h with increasing oA $\beta$ 1-42 concentrations (1, 5, or 10  $\mu\text{M}$ ), in the absence or presence of carnosine (Car, 1 mM) (oA $\beta$ 1-42 + Car (co-treat.)), or with a solution consisting of A $\beta$ 1-42 monomers previously incubated in the presence of carnosine (1 mM) during the oligomerization process (A $\beta$ 1-42 + Car (co-inc.)). Data are the mean of 5 independent experiments and are expressed as the percent variation with respect to the nitric oxide production recorded in resting cells. Standard deviations are represented by vertical bars. \*\* Significantly different from resting cells,  $p < 0.001$ , \*\*\* significantly different from corresponding treatment with no carnosine,  $p < 0.001$ .

As observed in the case of NO production, the stimulation of the cells with increasing concentration of oA $\beta$ 1-42 caused a dose-dependent increase in  $\text{O}_2^{\bullet-}$  production. This increase was significant in the case of both 5  $\mu\text{M}$  oA $\beta$ 1-42 (+43%,  $p < 0.001$  compared to resting cells) and 10  $\mu\text{M}$

oA $\beta$ 1-42 (+78%,  $p < 0.001$  compared to resting cells) treatments. A slight, but not significant, increase (+9%) compared to resting cells was measured in cells treated with 1  $\mu$ M oA $\beta$ 1-42. The addition of carnosine to resting BV-2 cells did not cause any significant change in the basal microglia O $_2^{\bullet-}$  production. To test the effect of carnosine on O $_2^{\bullet-}$  production in stimulated BV-2 cells, carnosine was added along with three different concentrations of oA $\beta$ 1-42. The amount of O $_2^{\bullet-}$  production was essentially the same for cells treated with 1  $\mu$ M oA $\beta$ 1-42, in the presence or absence of carnosine. The co-treatment with carnosine was able to counteract O $_2^{\bullet-}$  production in cell stimulated with 5  $\mu$ M oA $\beta$ 1-42 (−29%,  $p < 0.001$ ) as well as 10  $\mu$ M oA $\beta$ 1-42 (−53%,  $p < 0.001$ ). As for 1  $\mu$ M oA $\beta$ 1-42 + Car (co-treat.), the production of O $_2^{\bullet-}$  was essentially the same of the controls for A $\beta$ 1-42 1  $\mu$ M + Car (co-inc.). Once again, as previously observed for NO production, the presence of carnosine during the oligomerization process strongly decreased the effects of A $\beta$ 1-42 in inducing O $_2^{\bullet-}$  production. In fact, both 5  $\mu$ M A $\beta$ 1-42 + Car (co-inc.) (−34%,  $p < 0.001$ ) and 10  $\mu$ M A $\beta$ 1-42 + Car (co-inc.) (−60%,  $p < 0.001$ ) treatments showed a significant decrease in O $_2^{\bullet-}$  production when compared with the corresponding treatment in the absence of carnosine. A slight, but not significant, decrease (−9%) was measured for 1  $\mu$ M A $\beta$ 1-42 + Car (co-inc.) compared to the 1  $\mu$ M oA $\beta$ 1-42 treatment.

It is also worth underlining that in our experimental model the treatment of BV-2 cells with oA $\beta$ 1-42 produced more evident effects on O $_2^{\bullet-}$  production than those detected for NO production, at all concentrations (1, 5, or 10  $\mu$ M) tested.

By combining the information obtained from the first three sets of experiments (Figures 1–3), we selected the optimal oA $\beta$ 1-42 concentration (10  $\mu$ M) able to generate the strongest response in BV-2 cells, then used it, in the absence or presence of carnosine, to analyze mRNA expression and protein secretion.

#### 3.4. Carnosine Decreases A $\beta$ 1-42-Induced mRNA Expression Level of iNOS, Nox1, and Nox2 and Increases TGF- $\beta$ 1 mRNA Expression in Cultured Microglial Cells

Since the treatment of BV-2 cells with carnosine decreased the oA $\beta$ 1-42-induced production of NO and O $_2^{\bullet-}$  (Figures 2 and 3, respectively), we assessed the ability of carnosine to modulate the expression of iNOS and Nox subunits as well as the synthesis and the release of several cytokines related to A $\beta$ -induced inflammation in microglial cells. As expected, the expression level of iNOS mRNA was significantly increased (3.45 folds) following oA $\beta$ 1-42 treatment ( $p < 0.001$  compared to resting cells) (Figure 4A).

Both oA $\beta$ 1-42 + Car (co-treat.) and A $\beta$ 1-42 + Car (co-inc.) treatments were able to counteract A $\beta$ 1-42-induced iNOS activation ( $p < 0.001$  compared to oA $\beta$ 1-42-treated cells). The strongest inhibitory effect was observed for the A $\beta$ 1-42 + Car (co-inc.) treatment (from 3.45 folds to 1.09 folds) compared to the simple co-treatment with carnosine. The addition of carnosine to resting BV-2 cells did not cause any significant change in the expression level of iNOS mRNA. A slight, but not significant, increase (1.07 folds) was measured for Nox1 mRNA following oA $\beta$ 1-42 treatment, while values lower than the control were observed for oA $\beta$ 1-42 + Car (co-treat.) (0.91 folds) and A $\beta$ 1-42 + Car (co-inc.) (0.87 folds) treatments (Figure 4B). As observed for iNOS mRNA expression, the stimulation of BV-2 cells with oA $\beta$ 1-42 significantly increased the expression of Nox2 mRNA (1.96 folds,  $p < 0.001$ ) (Figure 4C). Both oA $\beta$ 1-42 + Car (co-treat.) and A $\beta$ 1-42 + Car (co-inc.) treatments gave values significantly lower than cells treated with A $\beta$ 1-42 in the absence of carnosine ( $p < 0.001$  compared to oA $\beta$ 1-42). Figure 4D shows the effect of A $\beta$ 1-42 treatment, alone or in combination with carnosine, on the expression level of TGF- $\beta$ 1 mRNA in BV-2 cells. A slight, but not significant, decrease (0.85 folds) was measured for TGF- $\beta$ 1 mRNA following oA $\beta$ 1-42 treatment. The co-treatment with carnosine increased the expression level to 1.09 folds ( $p < 0.05$  compared to oA $\beta$ 1-42-treated cells). For A $\beta$ 1-42 + Car (co-inc.) treatment the expression of TGF- $\beta$ 1 measured was equal to 1.30 folds ( $p < 0.01$  compared to resting cells;  $p < 0.001$  compared to oA $\beta$ 1-42-treated cells). Interestingly, carnosine per se provoked a significant increase (1.85 folds) in the expression level of TGF- $\beta$ 1 mRNA in resting BV-2 cells ( $p < 0.001$

compared to all other treatments). At this time point (6 h), the expression level of IL-6 mRNA in BV-2 cells did not significantly change in all the experimental conditions (data not shown).

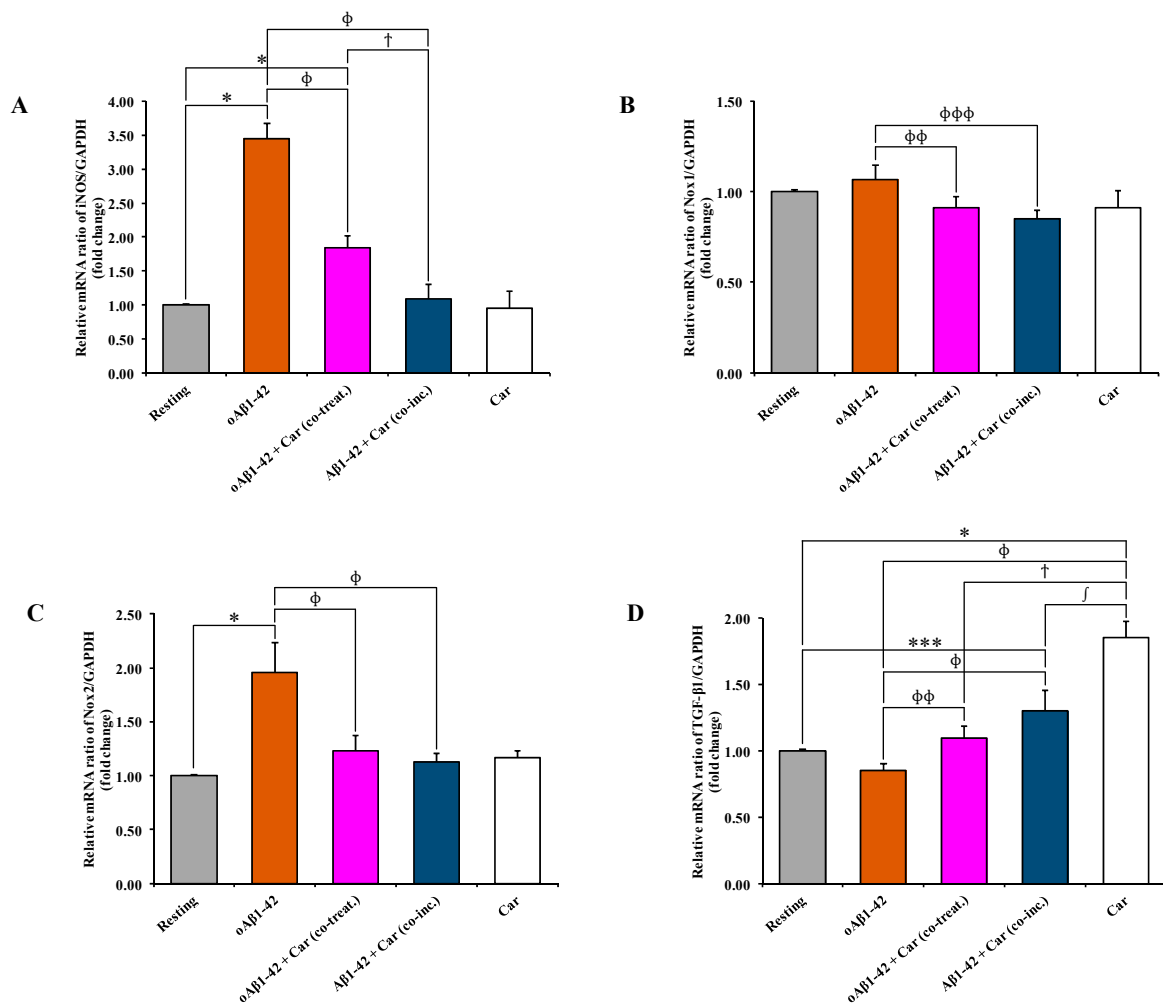


**Figure 4.** Carnosine suppresses the Aβ1-42-induced mRNA expression levels of iNOS, Nox1, and Nox2 and increases the expression of TGF-β1 mRNA. Effects of Aβ1-42 and carnosine (Aβ1-42 + Car (co-treat.) and Aβ1-42 + Car (co-inc.)) on (A) iNOS, (B) Nox1, (C) Nox2, and (D) TGF-β1 mRNAs expression were examined by qRT-PCR. The abundance of each mRNA of interest was expressed relative to the abundance of GAPDH-mRNA, as an internal control. As a negative control, a reaction in the absence of cDNA (no template control, NTC) was performed. qRT-PCR amplifications were performed in quadruplicate. Standard deviations are represented by vertical bars. \* significantly different from resting cells,  $p < 0.001$ , \*\* significantly different from resting cells,  $p < 0.05$ , \*\*\* significantly different from resting cells,  $p < 0.01$ ,  $\phi$  significantly different from oAβ1-42-treated cells,  $p < 0.001$ ,  $\phi\phi$  significantly different from oAβ1-42-treated cells,  $p < 0.05$ ,  $\phi\phi\phi$  significantly different from oAβ1-42-treated cells,  $p < 0.01$ ,  $\dagger$  significantly different from oAβ1-42 + Car (co-treat.)-treated cells,  $p < 0.001$ ,  $\ddagger$  significantly different from Aβ1-42 + Car (co-inc.)-treated cells,  $p < 0.001$ .

### 3.5. Carnosine Modulates the Release of Pro- and Anti-Inflammatory Cytokines in Cultured Microglial Cells

The analysis of cytokines in cell supernatants indicated an up-regulation (+15%) of the pro-inflammatory cytokine IL-1β induced by oAβ1-42 treatment compared to resting cells (Figure 5A).

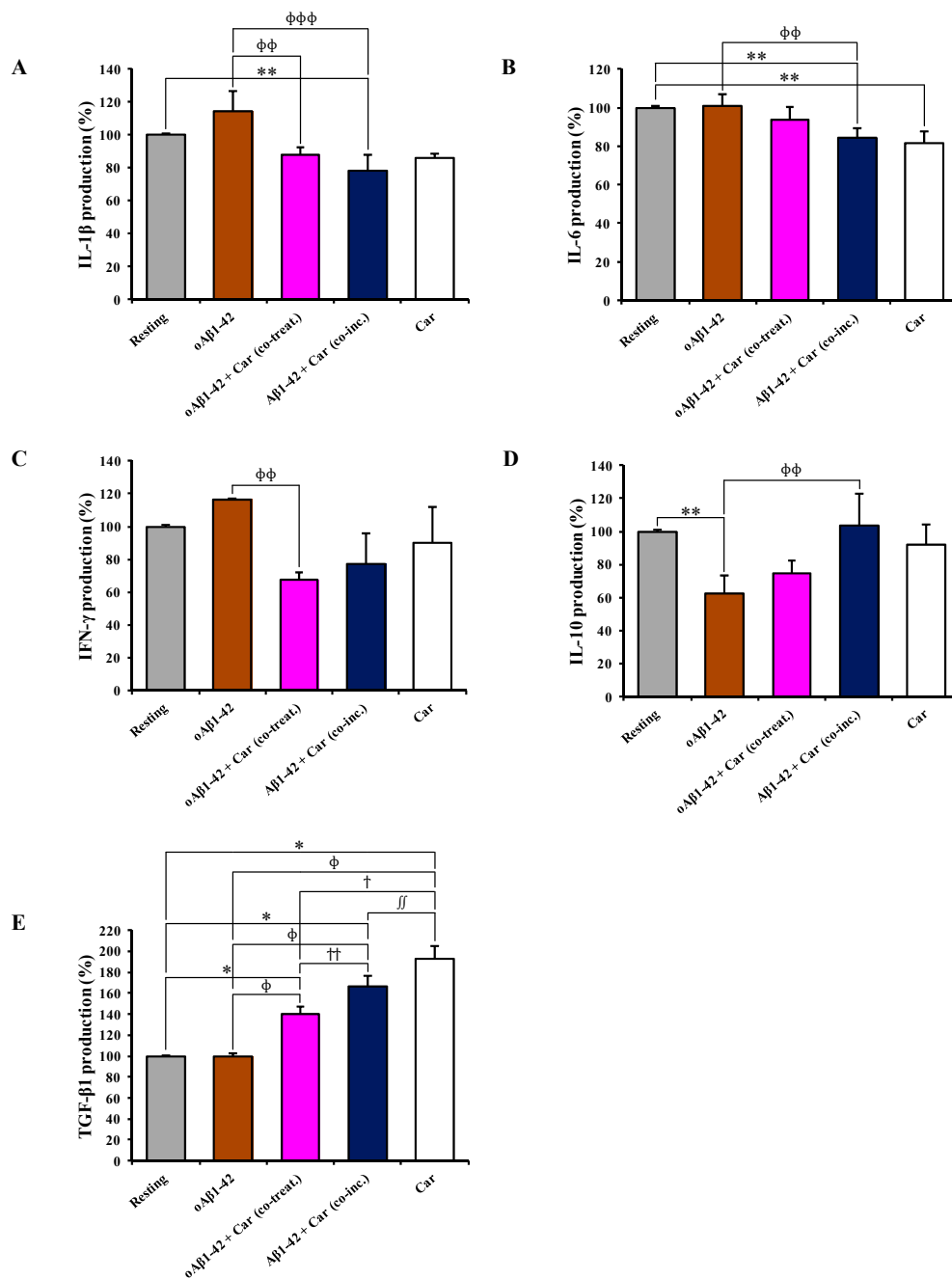


**Figure 5.** The modulation of cytokines secretion by carnosine. Supernatants from resting and BV-2 cells stimulated with oAβ1-42 in the absence or presence of carnosine (oAβ1-42 + Car (co-treat.) and Aβ1-42 + Car (co-inc.)) were analyzed using a Custom Multi-Analyte ELISArray Kit. Each treatment was analyzed in triplicate. The production of each cytokine is expressed as the percent variation with respect to the production recorded in resting cells. (A) IL-1β, (B) IL-6, (C) IFN-γ, (D) IL-10, and (E) TGF-β1. Standard deviations are represented by vertical bars. \* Significantly different from resting cells,  $p < 0.001$ , \*\* significantly different from resting cells,  $p < 0.05$ ,  $\phi$  significantly different from oAβ1-42-treated cells,  $p < 0.001$ ,  $\phi\phi$  significantly different from oAβ1-42-treated cells,  $p < 0.05$ ,  $\phi\phi\phi$  significantly different from oAβ1-42-treated cells,  $p < 0.01$ ,  $\dagger$  significantly different from oAβ1-42 + Car (co-treat.)-treated cells,  $p < 0.001$ ,  $\dagger\dagger$  significantly different from oAβ1-42 + Car (co-treat.)-treated cells,  $p < 0.05$ ,  $\int$  significantly different from Aβ1-42 + Car (co-inc.)-treated cells,  $p < 0.001$ ,  $\int\int$  significantly different from Aβ1-42 + Car (co-inc.)-treated cells,  $p < 0.05$ .

The presence of carnosine along with A $\beta$ 1-42 down-regulated the IL-1 $\beta$  production, with A $\beta$ 1-42 + Car (co-inc.) having a stronger effect (−36%,  $p < 0.001$  compared to oA $\beta$ 1-42-treated cells) than that of oA $\beta$ 1-42 + Car (co-treat.) (−27%,  $p < 0.05$  compared to oA $\beta$ 1-42-treated cells). The addition of carnosine to resting BV-2 cells did not cause any significant change in the release of IL-1 $\beta$ . The treatment of BV-2 cells with oA $\beta$ 1-42, alone or in co-treatment with carnosine, did not lead to any significant change in the production of the pro-inflammatory cytokine IL-6 (Figure 5B). On the contrary, both A $\beta$ 1-42 + Car (co-inc.) and carnosine alone treatments down-regulated IL-6 production ( $p < 0.05$  compared to resting and oA $\beta$ 1-42-treated cells and  $p < 0.05$  compared to resting, respectively). oA $\beta$ 1-42 treatment up-regulated IFN- $\gamma$  (+16%) in BV-2 cells (Figure 5C). Both treatments with carnosine down-regulated the IFN- $\gamma$  production compared to the corresponding treatment with no carnosine, with oA $\beta$ 1-42 + Car (co-treat.) treatment showing a stronger and significant effect (−33%,  $p < 0.05$  compared to oA $\beta$ 1-42-treated cells) than that of A $\beta$ 1-42 + Car (co-inc.) (−23%). The treatment with carnosine alone lowered IFN- $\gamma$  by 10%. Figure 5D,E shows the modulation in the release of the two major anti-inflammatory cytokines (IL-10 and TGF- $\beta$ 1) by A $\beta$ 1-42 in the absence or presence of carnosine. oA $\beta$ 1-42 treatment strongly down-regulated IL-10 production (−38%,  $p < 0.05$  compared to resting cells). oA $\beta$ 1-42 + Car (co-treat.) treatment slightly increased the production of IL-10 (+12%) while A $\beta$ 1-42 + Car (co-inc.) treatment rescued the IL-10 release to the values detected in resting cells, significantly higher than that of oA $\beta$ 1-42 alone (+41%,  $p < 0.05$ ) (Figure 5D). As in the case of IL-1 $\beta$ , the addition of carnosine to resting BV-2 cells did not cause any significant change in the release of IL-10. The level of TGF- $\beta$ 1 was very similar between resting and oA $\beta$ 1-42-treated BV-2 cells (Figure 5E). The treatment with carnosine along with oA $\beta$ 1-42 markedly up-regulated TGF- $\beta$ 1 (+40%,  $p < 0.001$  compared to resting and oA $\beta$ 1-42-treated cells) while the A $\beta$ 1-42 + Car (co-inc.) treatment led to an increase of TGF- $\beta$ 1 production equal to +66% compared to resting and oA $\beta$ 1-42-treated cells ( $p < 0.001$ ) and +26% compared to oA $\beta$ 1-42 + Car (co-treat.) treatment ( $p < 0.05$ ). Once again, as already observed for the expression level of TGF- $\beta$ 1 mRNA, the addition of carnosine per se to resting BV-2 cells strongly up-regulated the release of TGF- $\beta$ 1 (+93%,  $p < 0.05$  compared to A $\beta$ 1-42 + Car (co-inc.)-treated cells,  $p < 0.001$  compared to all other treatments).

### 3.6. Carnosine Prevents oA $\beta$ 1-42-Induced Toxicity in Mixed Neuronal Cultures via TGF- $\beta$ 1

Finally, we examined the neuroprotective activity of carnosine in mixed neuronal cultures containing both neurons (35–40%) and glial cells (astrocytes and microglia; 60–65%) challenged with oA $\beta$ 1-42 (2  $\mu$ M). We have previously demonstrated that mixed neuronal cultures treated with oA $\beta$ 1-42 represent an established experimental model of A $\beta$ -induced neurodegeneration, where oA $\beta$ 1-42 show a faster kinetics compared to pure neuronal cultures, with a substantial increase in the number of dead neurons (about 100%) being detected after 48 h of exposure to A $\beta$  oligomers [55].

Figure 6A clearly shows the neuroprotective effects of carnosine against oA $\beta$ 1-42-induced toxicity.

Carnosine decreased the oA $\beta$ 1-42 toxic effect in mixed neuronal cultures in a dose-dependent manner, with 10 mM carnosine (oA $\beta$ 1-42 + 10 mM Car) having a stronger protective effect (−55% in cell death,  $p < 0.001$  compared to oA $\beta$ 1-42 and oA $\beta$ 1-42 + 1 mM Car). The presence of carnosine at the final concentration of 1 or 5 mM reduced oA $\beta$ 1-42-induced cell death by 34% and 46%, respectively ( $p < 0.001$  compared to oA $\beta$ 1-42-treated cells). As shown in Figure 6B, the specific inhibitor of type-1 TGF- $\beta$  receptor, SB431542, prevented the neuroprotective activity of carnosine that was directly applied to mixed neuronal cultures challenged with oA $\beta$ 1-42 ( $p < 0.001$  compared to oA $\beta$ 1-42 + 10 mM Car) suggesting that TGF- $\beta$ 1 release and activation of TGF- $\beta$ 1 signaling play a central role in mediating the neuroprotective effects of carnosine. The percentage of toxicity due to the presence of oA $\beta$ 1-42 decreased by 53% (47% of cell death) in the presence of carnosine, but it increased again to a value very similar to oA $\beta$ 1-42 treatment in the presence of SB431542 (96% of cell death). The treatment with SB431542 (10  $\mu$ M) as well as with carnosine (10 mM) alone had no significant effects per se on neuronal death in mixed neuronal cultures in the absence of oA $\beta$ 1-42 treatment (Figure 6B, insert).

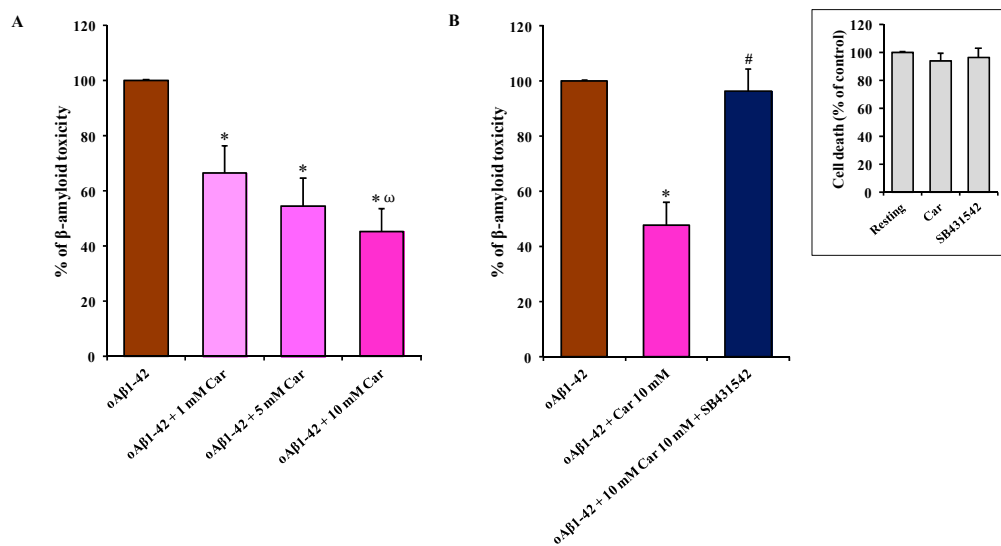


**Figure 6.** The neuroprotective effects of carnosine against oA $\beta$ 1-42-induced toxicity are mediated by TGF- $\beta$ 1. **(A)** Mixed neuronal cultures were challenged with oA $\beta$ 1-42 (2  $\mu$ M) for 48 h in the absence or presence of increasing concentrations of carnosine (1, 5, and 10 mM). **(B)** Effect of SB431542 (specific inhibitor of type-1 TGF- $\beta$  receptor) treatment (10  $\mu$ M) on the neuroprotective activity of carnosine against oA $\beta$ 1-42-induced toxicity. oA $\beta$ 1-42 toxicity in mixed neuronal cultures was assessed by cell counting after trypan blue staining. Cell counts were performed in three to four random microscopic fields/well. Data are the mean of 6 (A) or 5 (B) determinations and are expressed as the percent variation with respect to the cell death recorded in oA $\beta$ 1-42-treated cells. Standard deviations are represented by vertical bars. \* Significantly different from oA $\beta$ 1-42-treated cells,  $p < 0.001$ ,  $\omega$  significantly different from oA $\beta$ 1-42 + Car 1 mM,  $p < 0.001$ , # significantly different from oA $\beta$ 1-42 + Car 10 mM.

#### 4. Discussion

Oligomers, the most toxic species of A $\beta$ 1-42 aggregated forms, cause neuronal dysfunction and death in AD brains [56]. Microglial cells and neuronal cultures challenged with synthetic analogs of human oligomers of A $\beta$ 1-42 provide a widely accepted and reliable model of neuroinflammation and neurodegeneration occurring in AD [47,57,58]. In this scenario, oxidative stress plays a central role in A $\beta$ -induced neurodegeneration [59,60].

Oxidative stress is a process referring to an imbalance between pro-oxidants, such as ROS and RNS, and antioxidants in favor of pro-oxidants. A wide body of literature supports the negative impact and key role played by this phenomenon in the pathogenesis of AD [61], preceding the appearance of the two hallmarks of this disease represented by the abnormal deposition of A $\beta$  (senile plaques) and the intracellular accumulation of hyperphosphorylated tau protein (neurofibrillary tangles) [62]. In particular, on one hand the oligomeric form of A $\beta$  peptide impairs synaptic plasticity, and promotes neurodegeneration and neuroinflammation through oxidative stress [63,64]; on the other hand oxidative stress favors A $\beta$  oligomerization [65].

In the present study, we first explored the toxicity induced by different concentrations (1, 5, and 10  $\mu$ M) of A $\beta$ 1-42 oligomers on BV-2 microglial cells and then examined the correlation between A $\beta$  toxicity and the production of NO and O $_2^{\bullet-}$ , two well-known reactive species that significantly contribute to neurodegeneration in AD [66,67]. This order of magnitude ( $\mu$ M) is physiologically relevant since from one hand under normal physiological conditions and in AD patients the concentration of A $\beta$  peptide in brain extracellular fluid is low (pM to nM levels) [68–70]; on the other hand in vitro studies suggest that the critical concentration for spontaneous aggregation (e.g., oligomer formation) of A $\beta$  peptide is in the  $\mu$ M range [71,72]. Accordingly, A $\beta$  concentrations in vivo would have to increase by at least 3 to 4 orders of magnitude (e.g., close to the amyloid plaques) for spontaneous aggregation to be feasible in the extracellular space. When monitoring the change in

cell viability, we observed that oA $\beta$ 1-42 decreased BV-2 cell viability in a dose-dependent manner (Figure 1). BV-2 cells were able to counteract amyloid-induced cell toxicity only at low concentrations (1 or 5  $\mu$ M) while at the highest A $\beta$  concentration (10  $\mu$ M) the well-known ability of microglia in amyloid clearance [73] was overcome by A $\beta$  toxicity. Figure 1 also shows the protective effects of carnosine co-treatment in all the conditions tested. We hypothesized that these protective effects could be due to the ability of carnosine in counteracting both oxidative stress and inflammation in microglial cells [52,74]. In fact, as showed by Fleisher-Berkovich et al., carnosine as well as its acetylated form are able to decrease LPS-induced microglial oxidative stress and inflammation [74]. Furthermore, carnosine has been shown to protect neurons against oxidative stress by modulating the MAPK cascade signaling [3]. The neuroprotective effects exerted by carnosine have also been demonstrated by Lopachev et al. by using the primary culture of rat cerebellar cells under oxidative stress [75]. Our hypothesis was also strongly corroborated by the direct measurement of NO and O $_2^{\bullet-}$  intracellular levels as well as the expression of iNOS and Nox enzymes in A $\beta$ -stimulated cells. The levels of these reactive species increased in a dose-dependent manner by A $\beta$ 1-42 oligomers, whereas they significantly diminished in the presence of carnosine (Figures 2 and 3) in accordance to its antioxidant activity and the ability of this peptide to directly interact with these species, decreasing their availability [6,76]. In particular, part of the observed decreased toxicity could be due to an increased uptake of carnosine by immune cells under stress conditions [77], to the ability of this dipeptide to convert NO into its not-toxic end-product nitrite [6], and/or carnosine capability to disassemble aggregate structures already formed [78,79]. In accordance to the viability and NO and O $_2^{\bullet-}$  results, Figure 4A–C shows that the decrease in reactive species depends not only on the scavenging activity of carnosine [80] but also on the ability of this peptide to decrease the expression A $\beta$ -induced enzymes related to oxidative and nitrosative stress.

As a part of our study, instead of co-treating with carnosine and A $\beta$ 1-42 oligomers already formed, we challenged BV-2 cells with a solution consisting of A $\beta$ 1-42 monomers previously incubated in the presence of carnosine during the oligomerization process (indicated in each figure as A $\beta$ 1-42 + Car. (co-inc.)). Our aim was to determine whether the well-known anti-aggregation property of carnosine [81–83] contributed to decreasing the cell toxicity and oxidative stress by preventing the formation of A $\beta$ 1-42 toxic species. As expected, carnosine, by inhibiting oligomers formation (confirmed by AFM analysis (Supplementary Figure S1B), protected microglial cells (Figure 1), reduced NO (Figure 2) and O $_2^{\bullet-}$  (Figure 3) intracellular levels, and inhibited iNOS and Nox up-regulation (Figure 4A–C). These results are in accordance with Corona et al. which showed that carnosine supplementation in 3xTg-AD mice, a transgenic model of AD, led to a strong reduction in the hippocampal intraneuronal accumulation of A $\beta$ , completely rescuing AD and aging-related mitochondrial dysfunctions [4]. It is worth underlining that when considering the different protective effects observed between oA $\beta$ 1-42 + Car. (co-treat.) and A $\beta$ 1-42 + Car. (co-inc.) treatments, the latter gave always slightly stronger effects. The increased protective effect observed with carnosine in microglial cells after the co-incubation of A $\beta$  monomers with a millimolar concentration of carnosine suggests that the anti-aggregation properties of carnosine [5,78,79] significantly contribute to increase the overall protective effects of carnosine against A $\beta$ 1-42 toxicity in addition to the antioxidant activity of this peptide. Furthermore, our data obtained with AFM suggest that carnosine might preserve A $\beta$  monomers, which are essential for neuronal survival and maintaining neuronal glucose homeostasis [84,85], and it can also promote the dissociation of A $\beta$  oligomers. Future studies are needed to assess whether carnosine can act as a monomer stabilizer, preventing the transition from A $\beta$  monomers to A $\beta$  oligomers.

Activated microglia and astrocytes are the main source of cytokines in the brain [86], and elevated markers of microglial activation (measured by translocator protein binding in vivo with PET) have been found in AD patients [87]. A $\beta$  oligomers promote neuroinflammation and neurodegeneration in AD brains by eliciting the release of pro-inflammatory cytokines from microglia cells [88].

In the present study, we adopted an experimental model of neuroinflammation, where BV-2 microglial cells were challenged with a micromolar concentration of A $\beta$  oligomers [57,58]. A $\beta$ -induced inflammation in these cells is also known to strictly correlate with oxidative stress and an increase in ROS formation [89,90].

In our experimental model, A $\beta$  oligomers (24 h treatment) significantly reduced the secretion of anti-inflammatory cytokines such as IL-10 (Figure 5D), whereas no statistically significant effect was observed for IL-1 $\beta$  and IFN- $\gamma$  secretion (Figure 5A,C) as well as for IL-6 and TGF- $\beta$ 1 release (Figure 5B,E). With particular regard to IL-6, it is important to underline that differently from the gene expression analysis (6 h treatment), where the expression level of IL-6 mRNA was not changed by carnosine, cytokine secretion experiments (24 h treatment) demonstrate the ability of carnosine to decrease IL-6 levels. This suggests that under our experimental conditions: i) carnosine may require more than 6 h to directly modulate IL-6 gene expression; ii) carnosine could decrease IL-6 at post-translational level by direct interaction and/or modulating signal transduction pathways connected to its production such as phospholipases C and D [91]. Interestingly carnosine rescued IL-10 levels in A $\beta$ -treated BV-2 cells and also reduced IL-1 $\beta$ , IL-6, and IFN- $\gamma$  levels as assessed by the ELISA assay (Figure 5). Previous studies conducted *in vivo* have demonstrated that carnosine reduces both oxidative stress and microglial activation in animal models of subcortical ischemic vascular dementia and subarachnoid hemorrhage model [92–95], but no studies have been yet conducted in animal models of AD to examine the effects of carnosine on microglia activation. As discussed above, it is known from previous *in vitro* studies that carnosine can prevent LPS-induced microglial inflammation and oxidative damage [74], but our *in vitro* study is the first evidence that carnosine can counteract in microglial cells both oxidative stress and the release of pro-inflammatory cytokines induced by A $\beta$  oligomers. Furthermore, carnosine showed the ability to rescue IL-10 levels, an anti-inflammatory cytokine whose deficit in AD patients seems to play a key role in promoting neuroinflammation and cognitive deficits [96]. Future studies are needed to establish whether carnosine can exert this effect on IL-10 production *in vivo* in animal models of AD.

Interestingly we found that carnosine exerted a specific effect on the expression of TGF- $\beta$ 1, the only cytokine whose mRNA levels were significantly affected by carnosine with a relevant increase at 6 h (Figure 4D) followed by a strong increase in TGF- $\beta$ 1 release at 24 h (Figure 5E). We focused our attention on this anti-inflammatory cytokine because it is well-known that TGF- $\beta$ 1 exerts strong anti-inflammatory and neuroprotective effects in experimental models of AD [97]. It also plays a constitutive role in the suppression of inflammation, controlling the degree of microglial activation in the central nervous system [98] and stimulating A $\beta$  clearance by microglia [99]. It has also been recently demonstrated that microglial activation induced by A $\beta$ 1-42 oligomers results in the inhibition of TGF- $\beta$ -regulated gene expression in primary rat microglia [100]. When considering this evidence it is relevant to note that in our experimental model of A $\beta$ -induced inflammation carnosine was able to promote both the synthesis and the release of TGF- $\beta$ 1 from microglial cells. This effect of carnosine is relevant when taking into account the role of TGF- $\beta$ 1 in the pathophysiology of AD [101]. The selective impairment of the TGF- $\beta$ 1 signaling pathway has been demonstrated in the early phase of AD pathogenesis [102] and this deficit of TGF- $\beta$ 1 contributes to neuroinflammation and cognitive decline in AD [103]. Therefore, the rescue of TGF- $\beta$ 1 signaling represents a new pharmacological strategy to yield neuroprotection in AD and second-generation antidepressants such as fluoxetine increase the release of TGF- $\beta$ 1 from astrocytes and exert relevant neuroprotective effects in experimental models of AD [46].

Starting from this evidence, we examined the neuroprotective effects of carnosine in mixed neuronal cultures challenged with A $\beta$  oligomers, an established an experimental model of A $\beta$ -induced neurodegeneration [46,47]. Interestingly we found that carnosine started to prevent A $\beta$  toxicity at 1 mM, with a further relevant increase of its neuroprotective efficacy at 10 mM (with 55% of neuronal rescue) (Figure 6A). For our knowledge, this is the first evidence that carnosine can prevent A $\beta$ -induced neuronal death in an *in vitro* model of A $\beta$ -induced neurodegeneration. The protection



observed following carnosine treatment was in part expected since our results (Figures 4D and 5D,E) show that this dipeptide is able to enhance the ability of microglial cells to produce anti-inflammatory mediators (e.g., IL-10 and TGF- $\beta$ 1). According to this scenario, it is expected that the high percentage of glial cells (60–65%) in our co-culture model heavily contribute to neuronal protection. The ability of SB431542, a selective inhibitor of the type-1 TGF- $\beta$  receptor, to completely prevent the effects of carnosine (Figure 6B) suggests that TGF- $\beta$ 1 release and activation of Smad-dependent TGF- $\beta$ 1 signaling play key roles in mediating the neuroprotective efficacy of carnosine against A $\beta$  toxicity. Future studies should be conducted in transgenic animal models of AD to assess whether carnosine can prevent amyloid-related cognitive deficits by the rescue of TGF- $\beta$ 1 signaling.

## 5. Conclusions

In the present study, we reported for the first time that carnosine prevents A $\beta$ -induced oxidative stress in BV-2 microglial cells by decreasing the expression of inducible nitric oxide synthase and NADPH oxidase and the concentrations of nitric oxide and superoxide anion. We demonstrated for the first time that, in an established model of A $\beta$ -induced inflammation, carnosine was able to decrease the secretion of pro-inflammatory cytokines such as IL-1 $\beta$ , simultaneously rescuing IL-10 levels and increasing the synthesis and the release of TGF- $\beta$ 1. We then validated the protective activity of carnosine in mixed neuronal cultures challenged with A $\beta$ 1-42 oligomers, where carnosine prevented A $\beta$ -induced neurodegenerative phenomena via the activation of TGF- $\beta$ 1 signaling.

The inhibition of A $\beta$  oligomer-mediated inflammation and rescue of TGF- $\beta$ 1 signaling have been recently considered effective strategies for protecting against neurodegeneration and disease progression in AD. Carnosine, through its multimodal mechanism of action, might represent a new pharmacological tool to yield neuroprotection in AD.

**Supplementary Materials:** Supplementary materials can be found at <http://www.mdpi.com/2073-4409/8/1/64/s1>. Figure S1: AFM analysis of A $\beta$ 1-42 samples, Figure S2: A schematic representation of chip manufacturing process, ME-LIF setup, and representative electropherograms.

**Author Contributions:** Conceptualization, G.C., G.L. and F.C.; Validation, G.C., C.G.F. and N.M.; Formal Analysis, G.C., C.G.F., N.M., M.G. (Mariaconcetta Giambirtone), M.G. (Margherita Grasso), S.F.S. and S.M.; Investigation, G.C., C.G.F., N.M., M.G. (Mariaconcetta Giambirtone), M.G. (Margherita Grasso), S.F.S. and S.M.; Resources, M.A.S., F.D., S.M.L., G.L. and F.C.; Data Curation, G.C., C.G.F. and N.M.; Writing—Original Draft Preparation, G.C., C.G.F., N.M. and F.C.; Writing—Review & Editing, G.C., C.G.F., N.M., M.G. (Mariaconcetta Giambirtone), M.G. (Margherita Grasso), S.F.S., S.M., M.A.S., F.D., G.L. and F.C.; Visualization, G.C., C.G.F. and N.M.; Supervision, G.C., G.L. and F.C.; Project Administration, G.C., M.A.S., F.D., S.M.L., G.L. and F.C.; Funding Acquisition, G.C., S.M.L. and F.C.

**Funding:** Part of this study was supported by the National Science Foundation (NSF), grant number CHE-1411993, and National Institutes of Health (NIH), grant number COBRE P20GM103638. GC received support from the American Heart Association (Midwest Affiliate Postdoctoral Research Fellowship), grant number NFP0075515, while FC received support from the Neuropsychopharmacology Research Program 2017, grant number RC-06-05. GC and FC would also like to acknowledge the support received from the Italian Ministry of Health Research Program 2018, grant number RC: 2635256.

**Acknowledgments:** We would like to thank Dr. Gino Mongelli from BRIT for his valuable technician assistance during qRT-PCR and ELISA experiments and Dr. Vanna Torrisi from BRIT for help with AFM samples analysis.

**Conflicts of Interest:** The authors declare no conflict of interest.

## References

1. Quinn, P.J.; Boldyrev, A.A.; Formazuyk, V.E. Carnosine: Its properties, functions and potential therapeutic applications. *Mol. Asp. Med.* **1992**, *13*, 379–444. [[CrossRef](#)]
2. Hipkiss, A.R.; Brownson, C.; Bertani, M.F.; Ruiz, E.; Ferro, A. Reaction of carnosine with aged proteins: Another protective process? *Ann. N. Y. Acad. Sci.* **2002**, *959*, 285–294. [[CrossRef](#)] [[PubMed](#)]
3. Kulebyakin, K.; Karpova, L.; Lakonsteva, E.; Krasavin, M.; Boldyrev, A. Carnosine protects neurons against oxidative stress and modulates the time profile of mapk cascade signaling. *Amino Acids* **2012**, *43*, 91–96. [[CrossRef](#)] [[PubMed](#)]

4. Corona, C.; Frazzini, V.; Silvestri, E.; Lattanzio, R.; La Sorda, R.; Piantelli, M.; Canzoniero, L.M.; Ciavardelli, D.; Rizzarelli, E.; Sensi, S.L. Effects of dietary supplementation of carnosine on mitochondrial dysfunction, amyloid pathology, and cognitive deficits in 3xtg-ad mice. *PLoS ONE* **2011**, *6*, e17971. [[CrossRef](#)]
5. Aloisi, A.; Barca, A.; Romano, A.; Guerrieri, S.; Storelli, C.; Rinaldi, R.; Verri, T. Anti-aggregating effect of the naturally occurring dipeptide carnosine on abeta1-42 fibril formation. *PLoS ONE* **2013**, *8*, e68159. [[CrossRef](#)] [[PubMed](#)]
6. Caruso, G.; Fresta, C.G.; Martinez-Becerra, F.; Antonio, L.; Johnson, R.T.; de Campos, R.P.S.; Siegel, J.M.; Wijesinghe, M.B.; Lazzarino, G.; Lunte, S.M. Carnosine modulates nitric oxide in stimulated murine raw 264.7 macrophages. *Mol. Cell. Biochem.* **2017**, *431*, 197–210. [[CrossRef](#)] [[PubMed](#)]
7. Guliaeva, N.V. [Superoxide-scavenging activity of carnosine in the presence of copper and zinc ions]. *Biokhimiia* **1987**, *52*, 1216–1220.
8. Cripps, M.J.; Hanna, K.; Lavilla, C., Jr.; Sayers, S.R.; Caton, P.W.; Sims, C.; De Girolamo, L.; Sale, C.; Turner, M.D. Carnosine scavenging of glucolipotoxic free radicals enhances insulin secretion and glucose uptake. *Sci. Rep.* **2017**, *7*, 13313. [[CrossRef](#)]
9. Haass, C.; Schlossmacher, M.G.; Hung, A.Y.; Vigo-Pelfrey, C.; Mellon, A.; Ostaszewski, B.L.; Lieberburg, I.; Koo, E.H.; Schenk, D.; Teplow, D.B.; et al. Amyloid beta-peptide is produced by cultured cells during normal metabolism. *Nature* **1992**, *359*, 322–325. [[CrossRef](#)]
10. Sastre, M.; Klockgether, T.; Heneka, M.T. Contribution of inflammatory processes to alzheimer's disease: Molecular mechanisms. *Int. J. Dev. Neurosci.* **2006**, *24*, 167–176. [[CrossRef](#)]
11. Younkin, S.G. Evidence that a beta 42 is the real culprit in alzheimer's disease. *Ann. Neurol.* **1995**, *37*, 287–288. [[CrossRef](#)] [[PubMed](#)]
12. Haass, C.; Hung, A.Y.; Schlossmacher, M.G.; Oltersdorf, T.; Teplow, D.B.; Selkoe, D.J. Normal cellular processing of the beta-amyloid precursor protein results in the secretion of the amyloid beta peptide and related molecules. *Ann. N. Y. Acad. Sci.* **1993**, *695*, 109–116. [[CrossRef](#)] [[PubMed](#)]
13. Brion, J.P. Neurofibrillary tangles and alzheimer's disease. *Eur. Neurol.* **1998**, *40*, 130–140. [[CrossRef](#)] [[PubMed](#)]
14. Brorsson, A.C.; Kumita, J.R.; MacLeod, I.; Bolognesi, B.; Speretta, E.; Luheshi, L.M.; Knowles, T.P.; Dobson, C.M.; Crowther, D.C. Methods and models in neurodegenerative and systemic protein aggregation diseases. *Front. Biosci.* **2010**, *15*, 373–396.
15. Selkoe, D.J. Soluble oligomers of the amyloid beta-protein impair synaptic plasticity and behavior. *Behav. Brain Res.* **2008**, *192*, 106–113. [[CrossRef](#)] [[PubMed](#)]
16. Mittelbronn, M.; Dietz, K.; Schluesener, H.J.; Meyermann, R. Local distribution of microglia in the normal adult human central nervous system differs by up to one order of magnitude. *Acta Neuropathol.* **2001**, *101*, 249–255. [[PubMed](#)]
17. Kraft, A.D.; Harry, G.J. Features of microglia and neuroinflammation relevant to environmental exposure and neurotoxicity. *Int. J. Environ. Res. Public Health* **2011**, *8*, 2980–3018. [[CrossRef](#)]
18. Perlmutter, L.S.; Scott, S.A.; Barron, E.; Chui, H.C. Mhc class ii-positive microglia in human brain: Association with alzheimer lesions. *J. Neurosci. Res.* **1992**, *33*, 549–558. [[CrossRef](#)]
19. Wang, W.Y.; Tan, M.S.; Yu, J.T.; Tan, L. Role of pro-inflammatory cytokines released from microglia in alzheimer's disease. *Ann. Transl. Med.* **2015**, *3*, 136.
20. De Campos, R.P.; Siegel, J.M.; Fresta, C.G.; Caruso, G.; da Silva, J.A.; Lunte, S.M. Indirect detection of superoxide in raw 264.7 macrophage cells using microchip electrophoresis coupled to laser-induced fluorescence. *Anal. Bioanal. Chem.* **2015**, *407*, 7003–7012. [[CrossRef](#)]
21. Mainz, E.R.; Gunasekara, D.B.; Caruso, G.; Jensen, D.T.; Hulvey, M.K.; da Silva, J.A.F.; Metto, E.C.; Culbertson, A.H.; Culbertson, C.T.; Lunte, S.M. Monitoring intracellular nitric oxide production using microchip electrophoresis and laser-induced fluorescence detection. *Anal. Methods* **2012**, *4*, 414–420. [[CrossRef](#)]
22. Maes, M.; Galecki, P.; Chang, Y.S.; Berk, M. A review on the oxidative and nitrosative stress (O&NS) pathways in major depression and their possible contribution to the (NEURO)degenerative processes in that illness. *Prog. Neuropsychopharmacol. Biol. Psychiatry* **2011**, *35*, 676–692. [[PubMed](#)]
23. Fubini, B.; Hubbard, A. Reactive oxygen species (ROS) and reactive nitrogen species (RNS) generation by silica in inflammation and fibrosis. *Free Radic. Biol. Med.* **2003**, *34*, 1507–1516. [[CrossRef](#)]

24. Nakamura, T.; Lipton, S.A. Preventing Ca<sup>2+</sup>-mediated nitrosative stress in neurodegenerative diseases: Possible pharmacological strategies. *Cell Calcium* **2010**, *47*, 190–197. [[CrossRef](#)] [[PubMed](#)]
25. Kim, G.H.; Kim, J.E.; Rhie, S.J.; Yoon, S. The role of oxidative stress in neurodegenerative diseases. *Exp. Neurobiol.* **2015**, *24*, 325–340. [[CrossRef](#)] [[PubMed](#)]
26. Aktan, F. Inos-mediated nitric oxide production and its regulation. *Life Sci.* **2004**, *75*, 639–653. [[CrossRef](#)] [[PubMed](#)]
27. Metto, E.C.; Evans, K.; Barney, P.; Culbertson, A.H.; Gunasekara, D.B.; Caruso, G.; Hulvey, M.K.; Fracassi da Silva, J.A.; Lunte, S.M.; Culbertson, C.T. An integrated microfluidic device for monitoring changes in nitric oxide production in single t-lymphocyte (jurkat) cells. *Anal. Chem.* **2013**, *85*, 10188–10195. [[CrossRef](#)]
28. Sorescu, D.; Weiss, D.; Lassegue, B.; Clempus, R.E.; Szocs, K.; Sorescu, G.P.; Valppu, L.; Quinn, M.T.; Lambeth, J.D.; Vega, J.D.; et al. Superoxide production and expression of nox family proteins in human atherosclerosis. *Circulation* **2002**, *105*, 1429–1435. [[CrossRef](#)]
29. Mander, P.; Brown, G.C. Activation of microglial naph oxidase is synergistic with glial inos expression in inducing neuronal death: A dual-key mechanism of inflammatory neurodegeneration. *J. Neuroinflamm.* **2005**, *2*, 20. [[CrossRef](#)]
30. Siegel, J.M.; Schilly, K.M.; Wijesinghe, M.B.; Caruso, G.; Fresta, C.G.; Lunte, S.M. Optimization of a microchip electrophoresis method with electrochemical detection for the determination of nitrite in macrophage cells as an indicator of nitric oxide production. *Anal. Methods* **2019**, *11*, 148–156. [[CrossRef](#)]
31. Beckman, J.S.; Crow, J.P. Pathological implications of nitric oxide, superoxide and peroxynitrite formation. *Biochem. Soc. Trans.* **1993**, *21*, 330–334. [[CrossRef](#)] [[PubMed](#)]
32. Nakajima, K.; Kohsaka, S. Microglia: Activation and their significance in the central nervous system. *J. Biochem.* **2001**, *130*, 169–175. [[CrossRef](#)] [[PubMed](#)]
33. Lucherini, O.M.; Lopalco, G.; Cantarini, L.; Emmi, G.; Lopalco, A.; Venerito, V.; Vitale, A.; Iannone, F. Critical regulation of Th17 cell differentiation by serum amyloid-A signalling in Behcet’s disease. *Immunol Lett.* **2018**, *201*, 38–44. [[CrossRef](#)] [[PubMed](#)]
34. Lopalco, G.; Lucherini, O.M.; Lopalco, A.; Venerito, V.; Fabiani, C.; Frediani, B.; Galeazzi, M.; Lapadula, G.; Cantarini, L.; Iannone, F. Cytokine Signatures in Mucocutaneous and Ocular Behçet’s Disease. *Front. Immunol.* **2017**, *8*, 200. [[CrossRef](#)] [[PubMed](#)]
35. Heneka, M.T.; O’Banion, M.K.; Terwel, D.; Kummer, M.P. Neuroinflammatory processes in alzheimer’s disease. *J. Neural Transm.* **2010**, *117*, 919–947. [[CrossRef](#)] [[PubMed](#)]
36. Rojo, L.E.; Fernandez, J.A.; Maccioni, A.A.; Jimenez, J.M.; Maccioni, R.B. Neuroinflammation: Implications for the pathogenesis and molecular diagnosis of alzheimer’s disease. *Arch. Med. Res.* **2008**, *39*, 1–16. [[CrossRef](#)] [[PubMed](#)]
37. Smith, J.A.; Das, A.; Ray, S.K.; Banik, N.L. Role of pro-inflammatory cytokines released from microglia in neurodegenerative diseases. *Brain Res. Bull.* **2012**, *87*, 10–20. [[CrossRef](#)]
38. Schwab, C.; McGeer, P.L. Inflammatory aspects of alzheimer disease and other neurodegenerative disorders. *J. Alzheimers Dis.* **2008**, *13*, 359–369. [[CrossRef](#)]
39. Merlo, S.; Spampinato, S.F.; Beneventano, M.; Sortino, M.A. The contribution of microglia to early synaptic compensatory responses that precede  $\beta$ -amyloid-induced neuronal death. *Sci. Rep.* **2018**, *8*, 7297. [[CrossRef](#)]
40. Caraci, F.; Busceti, C.; Biagioni, F.; Aronica, E.; Mastroiacovo, F.; Cappuccio, I.; Battaglia, G.; Bruno, V.; Caricasole, A.; Copani, A.; et al. The wnt antagonist, dickkopf-1, as a target for the treatment of neurodegenerative disorders. *Neurochem. Res.* **2008**, *33*, 2401–2406. [[CrossRef](#)]
41. Caraci, F.; Spampinato, S.F.; Morgese, M.G.; Tascetta, F.; Salluzzo, M.G.; Giambirtone, M.C.; Caruso, G.; Munafo, A.; Torrisi, S.A.; Leggio, G.M.; et al. Neurobiological links between depression and ad: The role of tgf-beta1 signaling as a new pharmacological target. *Pharmacol. Res.* **2018**, *130*, 374–384. [[CrossRef](#)] [[PubMed](#)]
42. Luppi, C.; Fioravanti, M.; Bertolini, B.; Inguscio, M.; Grugnetti, A.; Guerriero, F.; Rovelli, C.; Cantoni, F.; Guagnano, P.; Marazzi, E.; et al. Growth factors decrease in subjects with mild to moderate alzheimer’s disease (AD): Potential correction with dehydroepiandrosterone-sulphate (DHEAS). *Arch. Gerontol. Geriatr.* **2009**, *49* (Suppl. 1), 173–184. [[CrossRef](#)] [[PubMed](#)]
43. Juraskova, B.; Andrys, C.; Holmerova, I.; Solichova, D.; Hrniciarikova, D.; Vankova, H.; Vasatko, T.; Krejsek, J. Transforming growth factor beta and soluble endoglin in the healthy senior and in alzheimer’s disease patients. *J. Nutr. Health Aging* **2010**, *14*, 758–761. [[CrossRef](#)] [[PubMed](#)]

44. Wyss-Coray, T.; Lin, C.; Yan, F.; Yu, G.Q.; Rohde, M.; McConlogue, L.; Masliah, E.; Mucke, L. TGF-beta1 promotes microglial amyloid-beta clearance and reduces plaque burden in transgenic mice. *Nat. Med.* **2001**, *7*, 612–618. [[CrossRef](#)] [[PubMed](#)]
45. Henn, A.; Lund, S.; Hedtjarn, M.; Schratzenholz, A.; Porzgen, P.; Leist, M. The suitability of BV2 cells as alternative model system for primary microglia cultures or for animal experiments examining brain inflammation. *Alz Dis.* **2009**, *26*, 83–94. [[CrossRef](#)] [[PubMed](#)]
46. Caraci, F.; Tascetta, F.; Merlo, S.; Benatti, C.; Spampinato, S.F.; Munafo, A.; Leggio, G.M.; Nicoletti, F.; Brunello, N.; Drago, F.; et al. Fluoxetine prevents abeta1-42-induced toxicity via a paracrine signaling mediated by transforming-growth-factor-beta1. *Front. Pharmacol.* **2016**, *7*, 389. [[CrossRef](#)] [[PubMed](#)]
47. Caraci, F.; Molinaro, G.; Battaglia, G.; Giuffrida, M.L.; Rizzo, B.; Traficante, A.; Bruno, V.; Cannella, M.; Merlo, S.; Wang, X.; et al. Targeting group ii metabotropic glutamate (mglu) receptors for the treatment of psychosis associated with alzheimer's disease: Selective activation of MGLU2 receptors amplifies beta-amyloid toxicity in cultured neurons, whereas dual activation of MGLU2 and MGLU3 receptors is neuroprotective. *Mol. Pharmacol.* **2011**, *79*, 618–626.
48. Caruso, G.; Fresta, C.G.; Lazzarino, G.; Distefano, D.A.; Parlascino, P.; Lunte, S.M.; Lazzarino, G.; Caraci, F. Sub-toxic human amylin fragment concentrations promote the survival and proliferation of SH-SY5Y cells via the release of VEGF and HSPB5 from endothelial RBE4 cells. *Int. J. Mol. Sci.* **2018**, *19*, 3659. [[CrossRef](#)]
49. Caruso, G.; Distefano, D.A.; Parlascino, P.; Fresta, C.G.; Lazzarino, G.; Lunte, S.M.; Nicoletti, V.G. Receptor-mediated toxicity of human amylin fragment aggregated by short- and long-term incubations with copper ions. *Mol. Cell. Biochem.* **2017**, *425*, 85–93. [[CrossRef](#)]
50. Caruso, G.; Fresta, C.G.; Siegel, J.M.; Wijesinghe, M.B.; Lunte, S.M. Microchip electrophoresis with laser-induced fluorescence detection for the determination of the ratio of nitric oxide to superoxide production in macrophages during inflammation. *Anal. Bioanal. Chem.* **2017**, *409*, 4529–4538. [[CrossRef](#)]
51. Gunasekara, D.B.; Siegel, J.M.; Caruso, G.; Hulvey, M.K.; Lunte, S.M. Microchip electrophoresis with amperometric detection method for profiling cellular nitrosative stress markers. *Analyst* **2014**, *139*, 3265–3273. [[CrossRef](#)] [[PubMed](#)]
52. Fresta, C.G.; Chakraborty, A.; Wijesinghe, M.B.; Amorini, A.M.; Lazzarino, G.; Lazzarino, G.; Tavazzi, B.; Lunte, S.M.; Caraci, F.; Dhar, P.; et al. Non-toxic engineered carbon nanodiamond concentrations induce oxidative/nitrosative stress, imbalance of energy metabolism, and mitochondrial dysfunction in microglial and alveolar basal epithelial cells. *Cell Death Dis.* **2018**, *9*, 245. [[CrossRef](#)] [[PubMed](#)]
53. Livak, K.J.; Schmittgen, T.D. Analysis of relative gene expression data using real-time quantitative pcr and the 2(-delta delta c(t)) method. *Methods* **2001**, *25*, 402–408. [[CrossRef](#)] [[PubMed](#)]
54. Barresi, V.; Ragusa, A.; Fichera, M.; Musso, N.; Castiglia, L.; Rappazzo, G.; Travali, S.; Mattina, T.; Romano, C.; Cocchi, G.; et al. Decreased expression of GRAF1/opln-1-1 in the x-linked alpha thalassemia mental retardation syndrome. *BMC Med. Genom.* **2010**, *3*, 28. [[CrossRef](#)] [[PubMed](#)]
55. Caraci, F.; Pappalardo, G.; Basile, L.; Giuffrida, A.; Copani, A.; Tosto, R.; Sinopoli, A.; Giuffrida, M.L.; Pirrone, E.; Drago, F.; et al. Neuroprotective effects of the monoamine oxidase inhibitor tranylcypromine and its amide derivatives against abeta(1-42)-induced toxicity. *Eur. J. Pharmacol.* **2015**, *764*, 256–263. [[CrossRef](#)] [[PubMed](#)]
56. Klein, W.L. Synaptotoxic amyloid-beta oligomers: A molecular basis for the cause, diagnosis, and treatment of alzheimer's disease? *J. Alzheimers Dis.* **2013**, *33* (Suppl. 1), S49–S65. [[CrossRef](#)] [[PubMed](#)]
57. Jiao, C.; Gao, F.; Ou, L.; Yu, J.; Li, M.; Wei, P.; Miu, F. Tetrahydroxystilbene glycoside antagonizes beta-amyloid-induced inflammatory injury in microglia cells by regulating pu.1 expression. *Neuroreport* **2018**, *29*, 787–793. [[CrossRef](#)]
58. Ries, M.; Loiola, R.; Shah, U.N.; Gentleman, S.M.; Solito, E.; Sastre, M. The anti-inflammatory annexin a1 induces the clearance and degradation of the amyloid-beta peptide. *J. Neuroinflamm.* **2016**, *13*, 234. [[CrossRef](#)]
59. Butterfield, D.A. Amyloid beta-peptide (1-42)-induced oxidative stress and neurotoxicity: Implications for neurodegeneration in alzheimer's disease brain. A review. *Free Radic. Res.* **2002**, *36*, 1307–1313. [[CrossRef](#)]
60. Cheignon, C.; Tomas, M.; Bonnefont-Rousselot, D.; Faller, P.; Hureau, C.; Collin, F. Oxidative stress and the amyloid beta peptide in alzheimer's disease. *Redox Biol.* **2018**, *14*, 450–464. [[CrossRef](#)]
61. Serini, S.; Calviello, G. Reduction of oxidative/nitrosative stress in brain and its involvement in the neuroprotective effect of n-3 pufa in alzheimer's disease. *Curr. Alzheimer Res.* **2016**, *13*, 123–134. [[CrossRef](#)] [[PubMed](#)]

62. Huang, W.J.; Zhang, X.; Chen, W.W. Role of oxidative stress in alzheimer's disease. *Biomed. Rep.* **2016**, *4*, 519–522. [[CrossRef](#)] [[PubMed](#)]
63. Gelain, D.P.; Antonio Behr, G.; Birnfeld de Oliveira, R.; Trujillo, M. Antioxidant therapies for neurodegenerative diseases: Mechanisms, current trends, and perspectives. *Oxid. Med. Cell. Longev.* **2012**, *2012*, 895153. [[CrossRef](#)] [[PubMed](#)]
64. Varadarajan, S.; Yatin, S.; Aksenova, M.; Butterfield, D.A. Review: Alzheimer's amyloid beta-peptide-associated free radical oxidative stress and neurotoxicity. *J. Struct. Biol.* **2000**, *130*, 184–208. [[CrossRef](#)] [[PubMed](#)]
65. Zhao, Y.; Zhao, B. Oxidative stress and the pathogenesis of alzheimer's disease. *Oxid. Med. Cell. Longev.* **2013**, *2013*, 316523. [[CrossRef](#)] [[PubMed](#)]
66. Togo, T.; Katsuse, O.; Iseki, E. Nitric oxide pathways in alzheimer's disease and other neurodegenerative dementias. *Neurol. Res.* **2004**, *26*, 563–566. [[CrossRef](#)] [[PubMed](#)]
67. Massaad, C.A.; Pautler, R.G.; Klann, E. Mitochondrial superoxide: A key player in alzheimer's disease. *Aging* **2009**, *1*, 758–761. [[CrossRef](#)] [[PubMed](#)]
68. Hu, X.; Crick, S.L.; Bu, G.; Frieden, C.; Pappu, R.V.; Lee, J.M. Amyloid seeds formed by cellular uptake, concentration, and aggregation of the amyloid-beta peptide. *Proc. Natl. Acad. Sci. USA* **2009**, *106*, 20324–20329. [[CrossRef](#)]
69. Seubert, P.; Vigo-Pelfrey, C.; Esch, F.; Lee, M.; Dovey, H.; Davis, D.; Sinha, S.; Schlossmacher, M.; Whaley, J.; Swindlehurst, C.; et al. Isolation and quantification of soluble Alzheimer's beta-peptide from biological fluids. *Nature* **1992**, *359*, 325–327. [[CrossRef](#)]
70. Strozyk, D.; Blennow, K.; White, L.R.; Launer, L.J. CSF Aβ42 levels correlate with amyloid-neuropathology in a population-based autopsy study. *Neurology* **2003**, *60*, 652–656. [[CrossRef](#)]
71. Harper, J.D.; Wong, S.S.; Lieber, C.M.; Lansbury, P.T. Jr. Assembly of Aβ42 amyloid protofibrils: An in vitro model for a possible early event in Alzheimer's disease. *Biochemistry* **1999**, *38*, 8972–8980. [[CrossRef](#)] [[PubMed](#)]
72. Lomakin, A.; Teplow, D.B.; Kirschner, D.A.; Benedek, G.B. Kinetic theory of fibrillogenesis of amyloid beta-protein. *Proc. Natl. Acad. Sci. USA* **1997**, *94*, 7942–7947. [[CrossRef](#)] [[PubMed](#)]
73. Lai, A.Y.; McLaurin, J. Clearance of amyloid-beta peptides by microglia and macrophages: The issue of what, when and where. *Future Neurol.* **2012**, *7*, 165–176. [[CrossRef](#)] [[PubMed](#)]
74. Fleisher-Berkovich, S.; Abramovitch-Dahan, C.; Ben-Shabat, S.; Apte, R.; Beit-Yannai, E. Inhibitory effect of carnosine and n-acetyl carnosine on Iβs-induced microglial oxidative stress and inflammation. *Peptides* **2009**, *30*, 1306–1312. [[CrossRef](#)] [[PubMed](#)]
75. Lopachev, A.V.; Lopacheva, O.M.; Abaimov, D.A.; Koroleva, O.V.; Vladychenskaya, E.A.; Erukhimovich, A.A.; Fedorova, T.N. Neuroprotective effect of carnosine on primary culture of rat cerebellar cells under oxidative stress. *Biochemistry* **2016**, *81*, 511–520. [[CrossRef](#)] [[PubMed](#)]
76. Klebanov, G.I.; Teselkin Yu, O.; Babenkova, I.V.; Popov, I.N.; Levin, G.; Tyulina, O.V.; Boldyrev, A.A.; Vladimirov Yu, A. Evidence for a direct interaction of superoxide anion radical with carnosine. *Biochem. Mol. Biol. Int.* **1997**, *43*, 99–106. [[CrossRef](#)] [[PubMed](#)]
77. Fresta, C.G.; Hogard, M.L.; Caruso, G.; Melo Costa, E.E.; Lazzarino, G.; Lunte, S.M. Monitoring carnosine uptake by raw 264.7 macrophage cells using microchip electrophoresis with fluorescence detection. *Anal. Methods* **2017**, *9*, 402–408. [[CrossRef](#)] [[PubMed](#)]
78. Attanasio, F.; Cataldo, S.; Fisichella, S.; Nicoletti, S.; Nicoletti, V.G.; Pignataro, B.; Savarino, A.; Rizzarelli, E. Protective effects of l- and d-carnosine on alpha-crystallin amyloid fibril formation: Implications for cataract disease. *Biochemistry* **2009**, *48*, 6522–6531. [[CrossRef](#)]
79. Javadi, S.; Yousefi, R.; Hosseinkhani, S.; Tamaddon, A.M.; Uversky, V.N. Protective effects of carnosine on dehydroascorbate-induced structural alteration and opacity of lens crystallins: Important implications of carnosine pleiotropic functions to combat cataractogenesis. *J. Biomol. Struct. Dyn.* **2017**, *35*, 1766–1784. [[CrossRef](#)]
80. Salim-Hanna, M.; Lissi, E.; Videla, L.A. Free radical scavenging activity of carnosine. *Free Radic. Res. Commun.* **1991**, *14*, 263–270. [[CrossRef](#)]
81. Hipkiss, A.R.; Michaelis, J.; Syrris, P. Non-enzymatic glycosylation of the dipeptide l-carnosine, a potential anti-protein-cross-linking agent. *FEBS Lett.* **1995**, *371*, 81–85. [[CrossRef](#)]

82. Grasso, G.I.; Bellia, F.; Arena, G.; Satriano, C.; Vecchio, G.; Rizzarelli, E. Multitarget trehalose-carnosine conjugates inhibit abeta aggregation, tune copper(ii) activity and decrease acrolein toxicity. *Eur. J. Med. Chem.* **2017**, *135*, 447–457. [[CrossRef](#)] [[PubMed](#)]
83. Attanasio, F.; Convertino, M.; Magno, A.; Cafilisch, A.; Corazza, A.; Haridas, H.; Esposito, G.; Cataldo, S.; Pignataro, B.; Milardi, D.; et al. Carnosine inhibits abeta(42) aggregation by perturbing the h-bond network in and around the central hydrophobic cluster. *Chembiochem* **2013**, *14*, 583–592. [[CrossRef](#)] [[PubMed](#)]
84. Giuffrida, M.L.; Caraci, F.; De Bona, P.; Pappalardo, G.; Nicoletti, F.; Rizzarelli, E.; Copani, A. The monomer state of beta-amyloid: Where the alzheimer's disease protein meets physiology. *Rev. Neurosci.* **2010**, *21*, 83–93. [[CrossRef](#)] [[PubMed](#)]
85. Giuffrida, M.L.; Tomasello, M.F.; Pandini, G.; Caraci, F.; Battaglia, G.; Busceti, C.; Di Pietro, P.; Pappalardo, G.; Attanasio, F.; Chiechio, S.; et al. Monomeric ss-amyloid interacts with type-1 insulin-like growth factor receptors to provide energy supply to neurons. *Front. Cell. Neurosci.* **2015**, *9*, 297. [[CrossRef](#)] [[PubMed](#)]
86. Hashioka, S.; Miyaoka, T.; Wake, R.; Furuya, M.; Horiguchi, J. Glia: An important target for anti-inflammatory and antidepressant activity. *Curr. Drug Targets* **2013**, *14*, 1322–1328. [[CrossRef](#)] [[PubMed](#)]
87. Knezevic, D.; Mizrahi, R. Molecular imaging of neuroinflammation in alzheimer's disease and mild cognitive impairment. *Prog. Neuropsychopharmacol. Biol. Psychiatry* **2018**, *80*, 123–131. [[CrossRef](#)]
88. Businaro, R.; Corsi, M.; Asprino, R.; Di Lorenzo, C.; Laskin, D.; Corbo, R.M.; Ricci, S.; Pinto, A. Modulation of inflammation as a way of delaying alzheimer's disease progression: The diet's role. *Curr. Alzheimer Res.* **2018**, *15*, 363–380. [[CrossRef](#)]
89. Pangestuti, R.; Vo, T.S.; Ngo, D.H.; Kim, S.K. Fucoxanthin ameliorates inflammation and oxidative responses in microglia. *J. Agric. Food Chem.* **2013**, *61*, 3876–3883. [[CrossRef](#)]
90. Correani, V.; Di Francesco, L.; Cera, I.; Mignogna, G.; Giorgi, A.; Mazzanti, M.; Fumagalli, L.; Fabrizi, C.; Maras, B.; Schinina, M.E. Reversible redox modifications in the microglial proteome challenged by beta amyloid. *Mol. Biosyst.* **2015**, *11*, 1584–1593. [[CrossRef](#)]
91. Hatakeyama, D.; Kozawa, O.; Otsuka, T.; Shibata, T.; Uematsu, T. Zinc suppresses IL-6 synthesis by prostaglandin F2alpha in osteoblasts: Inhibition of phospholipase C and phospholipase D. *J. Cell. Biochem.* **2002**, *85*, 621–628. [[CrossRef](#)] [[PubMed](#)]
92. Ma, J.; Yan, H.; Wang, R.; Bo, S.; Lu, X.; Zhang, J.; Xu, A. Protective effect of carnosine on white matter damage in corpus striatum induced by chronic cerebral hypoperfusion. *Neurosci. Lett.* **2018**, *683*, 54–60. [[CrossRef](#)] [[PubMed](#)]
93. Xie, R.X.; Li, D.W.; Liu, X.C.; Yang, M.F.; Fang, J.; Sun, B.L.; Zhang, Z.Y.; Yang, X.Y. Carnosine attenuates brain oxidative stress and apoptosis after intracerebral hemorrhage in rats. *Neurochem. Res.* **2017**, *42*, 541–551. [[CrossRef](#)] [[PubMed](#)]
94. Zhang, Z.Y.; Sun, B.L.; Yang, M.F.; Li, D.W.; Fang, J.; Zhang, S. Carnosine attenuates early brain injury through its antioxidative and anti-apoptotic effects in a rat experimental subarachnoid hemorrhage model. *Cell. Mol. Neurobiol.* **2015**, *35*, 147–157. [[CrossRef](#)]
95. Ma, J.; Xiong, J.Y.; Hou, W.W.; Yan, H.J.; Sun, Y.; Huang, S.W.; Jin, L.; Wang, Y.; Hu, W.W.; Chen, Z. Protective effect of carnosine on subcortical ischemic vascular dementia in mice. *CNS Neurosci. Ther.* **2012**, *18*, 745–753. [[CrossRef](#)] [[PubMed](#)]
96. Magalhaes, C.A.; Carvalho, M.D.G.; Sousa, L.P.; Caramelli, P.; Gomes, K.B. Alzheimer's disease and cytokine il-10 gene polymorphisms: Is there an association? *Arq Neuropsiquiatr.* **2017**, *75*, 649–656. [[CrossRef](#)] [[PubMed](#)]
97. Chen, J.H.; Ke, K.F.; Lu, J.H.; Qiu, Y.H.; Peng, Y.P. Protection of tgf-beta1 against neuroinflammation and neurodegeneration in abeta1-42-induced alzheimer's disease model rats. *PLoS ONE* **2015**, *10*, e0116549.
98. Brionne, T.C.; Tesseur, I.; Masliah, E.; Wyss-Coray, T. Loss of TGF-beta 1 leads to increased neuronal cell death and microgliosis in mouse brain. *Neuron* **2003**, *40*, 1133–1145. [[CrossRef](#)]
99. Tichauer, J.E.; Flores, B.; Soler, B.; Eugenin-von Bernhardt, L.; Ramirez, G.; von Bernhardt, R. Age-dependent changes on TGF-beta1 SMAD3 pathway modify the pattern of microglial cell activation. *Brain Behav. Immun.* **2014**, *37*, 187–196. [[CrossRef](#)]
100. Affram, K.O.; Mitchell, K.; Symes, A.J. Microglial activation results in inhibition of tgf-beta-regulated gene expression. *J. Mol. Neurosci.* **2017**, *63*, 308–319. [[CrossRef](#)]

101. Caruso, G.; Caraci, F.; Jolivet, R.B. Pivotal role of carnosine in the modulation of brain cells activity: Multimodal mechanism of action and therapeutic potential in neurodegenerative disorders. *Prog. Neurobiol.* **2018**. [[CrossRef](#)] [[PubMed](#)]
102. Tesseur, I.; Zou, K.; Esposito, L.; Bard, F.; Berber, E.; Can, J.V.; Lin, A.H.; Crews, L.; Tremblay, P.; Mathews, P.; et al. Deficiency in neuronal tgf-beta signaling promotes neurodegeneration and alzheimer's pathology. *J. Clin. Investig.* **2006**, *116*, 3060–3069. [[CrossRef](#)] [[PubMed](#)]
103. Caraci, F.; Gili, E.; Calafiore, M.; Failla, M.; La Rosa, C.; Crimi, N.; Sortino, M.A.; Nicoletti, F.; Copani, A.; Vancheri, C. TGF-beta1 targets the GSK-3beta/beta-catenin pathway via ERK activation in the transition of human lung fibroblasts into myofibroblasts. *Pharmacol. Res.* **2008**, *57*, 274–282. [[CrossRef](#)] [[PubMed](#)]



© 2019 by the authors. Licensee MDPI, Basel, Switzerland. This article is an open access article distributed under the terms and conditions of the Creative Commons Attribution (CC BY) license (<http://creativecommons.org/licenses/by/4.0/>).